Oxford Open Climate Change, 2023, **3(1),** kgad004
https://doi.org/10.1093/oxfclm/kgad004
Advance Access Publication Date: 21 April 2023
Review

Marine methods for carbon dioxide removal: fundamentals and myth-busting for the wider community

Eelco J. Rohling [1,2,*]

[1]Research School of Earth Sciences, Australian National University, Canberra, ACT 2600, Australia
[2]Ocean and Earth Science, National Oceanography Centre, University of Southampton, Southampton SO14 3ZH, UK

*Correspondence address. Research School of Earth Sciences, Australian National University, Canberra, ACT, Australia. E-mail: eelco.rohling@anu.edu.au

Abstract

To avoid global warming in excess of 1.5°C under the current sluggish adoption of drastic reductions in global greenhouse gas emissions, application of methods to remove carbon dioxide from the atmosphere will become essential in the near future; yet, development of these methods is in its infancy. Land-based methods are further developed than marine methods, but it is likely that similar-scaled application will be necessary in both realms. There are many misconceptions in discussion groups and fora about the 'simplicity' or 'ease' of proposed marine applications, partly because the complex marine carbon cycle is insufficiently understood by the proponents, having been discussed in largely inaccessible, technical texts only. This review outlines the basic operation of the marine carbon cycle in straightforward terms, with some simplifications, to help advance the debate among the wider community. Break-out boxes provide additional detail where desired, and references (and the sources cited therein) provide avenues for further study. The review then discusses two potential marine methods for atmospheric carbon removal that are thought to offer the greatest potential in terms of carbon removal mass: ocean iron fertilization and ocean alkalinity enhancement. Finally, six statements/arguments that seem to regularly crop up in carbon removal discussion groups are evaluated within the perspective of the compiled and reviewed information.

Keywords: marine; carbon dioxide; removal; fundamentals; myth-busting

INTRODUCTION

With every passing year of continuing, unabated emissions, the likelihood of failure to limit global warming to 1.5°C above pre-industrial levels through net-zero emissions alone is rapidly increasing [1]. This realization is driving a wave of interest in methods for greenhouse gas removal from the climate system. With respect to carbon, the focus of this review, these are described in various guises as negative emissions technologies, carbon sequestration (CS) and carbon dioxide (CO_2) removal approaches. These methods target removal of carbon (CO_2 and/or CH_4) from the atmosphere, 'locking it away' for long periods of time (in excess of several centuries) in a wide variety of semi-permanent 'reservoirs' (for overviews, see Refs [2–4]).

During pre-industrial history, the ocean dominated atmospheric CO_2 concentrations because it contains ~60 times more carbon and because natural dynamics of CO_2 exchange between the ocean and atmosphere were slow enough. In fact, the ocean is the largest reservoir of carbon after sedimentary rocks. As a result, there is a lot of interest in potential atmospheric carbon removal using long-term storage in the ocean. Not all methods are about improved carbon uptake into the ocean—methods that aim to 'switch off' long-standing sources of carbon outgassing from the ocean into the atmosphere are equally important. Essentially, some methods aim to add carbon into the oceanic reservoir, while others aim to prevent escape of carbon from the oceanic reservoir; both increase net carbon storage in the ocean There is particular interest in methods that use ocean chemistry, physics and/or biology for CO_2 capture and then store it for multi-centennial to millennial timescales in the deep-sea, or permanently in seafloor sediments. Although total atmospheric carbon removal potential for marine methods is very uncertain, two of these methods are often listed as having the greatest atmospheric carbon removal potentials: (i) ocean iron fertilization and (ii) ocean alkalinity enhancement (OAE) [2–4]. These methods will be discussed in more detail toward the end of this paper. A third method that receives quite a lot of attention is artificial upwelling, but its carbon removal potential is still thought to be much lower than that of the other two methods (see synthesis in Ref. [4]); hence, it is not included in the discussion here. In addition, the two methods discussed already highlight the main benefits, feedbacks and side-effects that need to be considered with all marine methods.

Participation to atmospheric carbon removal discussion groups (e.g. carbondioxideremoval@googlegroups.com) has revealed a lively debate among researchers, engineers, inventors, entrepreneurs and engaged members of the public on atmospheric carbon removal methods, their potentials and their impacts. Yet, it has also revealed that ocean-focused ideas and

Received: November 18, 2022. **Revised:** April 17, 2023. **Accepted:** April 19, 2023

concepts (which sometimes include calls for immediate implementation) often would be well-served by a deeper appreciation of the oceanic carbon cycle, and especially of the intricate feedbacks and interdependences between biological and a-biological carbon cycling that affect the efficacies and potential side-effects of the ideas proposed. The oceanic carbon cycle is among the most challenging topics in oceanography, and most available literature is highly technical. To assist the wider community interested in oceanic methods for atmospheric carbon removal, this paper reviews and synthesizes the essence of the marine carbon cycle in straightforward terms (with some simplifications), while providing key references to guide further in-depth study. It will specifically address a series of statements or arguments that seem to come up rather frequently in carbon drawdown discussion groups, namely:

1) Oceanic CO_2 uptake with changing temperature may be calculated simply with physical solubility arguments.
2) Carbonate formation should be promoted because it causes carbon drawdown.
3) Ocean iron fertilization will draw down carbon and store it in increased fish populations (which are commercially interesting).
4) Ocean iron fertilization has only positive (enriching) side-effects.
5) Enhanced primary production will be buried in sediments without major detrimental impacts.
6) Impacts of regionally applied methods in the ocean can be confined to that region.

This review outlines the nature of the system that proposed methods aim to influence, and highlights the types of (sometimes far-reaching) trade-offs and side-effects that need to be considered. It starts with an overview of the fundamental bio-geo-chemical reactions that govern the physical, chemical and biological controls on carbon movements through the ocean, and of the key interactions between these controls (Sections 'Fundamentals', 'Spatial property distributions' and 'Vertical gradients—carbon transport into the ocean interior'). Then follows a discussion of two main oceanic methods for atmospheric carbon removal, along with their immediate drawbacks and potential for unexpected, remote or delayed side-effects (Section 'Using ocean biogeochemistry to mitigate CO_2 emissions'). Finally, the compiled information is used to debunk the above six frequent statements/arguments collected from carbon drawdown discussion groups (Section 'Debunking frequently encountered statements/arguments'). The article does not go into detail about ecological consequences (such as species-dominance changes, bio-physical adaptation pressures, food-web changes and foreign species invasion), as these are highly application and location specific. Most numbers and concentrations reported in this article are indicative rather than precise; for precise numbers, rigorous corrections to standard reference conditions would need to be made throughout, but the core arguments made here are not affected.

FUNDAMENTALS

For detailed descriptions of the reactions and interactions involved in the marine carbon cycle, see the overviews of Refs [5–12], and their cited sources.

Molecules of CO_2 (as for any gas) continually cross the air–sea interface; the flows into and out of the water are known as fluxes. When influx and outflux are identical, then the air and water gas reservoirs are said to be in equilibrium. The abundance of atmospheric CO_2 is expressed in terms of its partial pressure in dry air; i.e. after removal of all water vapor (pCO_2^{atm}, in micro-atmospheres, μatm). The concentration of non-ionized CO_2 dissolved in sea water is indicated with $[CO_2]$, where the square brackets indicate 'concentrations of' and the units are μmol kg^{-1}. Finally, measurement of pCO_2 in water (pCO_2^w) is not possible in a similar manner to the measurement of pCO_2^{atm}, and pCO_2^w is instead defined as the pCO_2^{atm} that would be reached if there were a perfect equilibrium with $[CO_2]$ (Henry's Law; [13]). The equilibrium relationship between $[CO_2]$ and pCO_2^w is determined by K_0, the largely temperature-dependent and somewhat salinity-dependent solubility of CO_2: $K_0 = [CO_2]/pCO_2^w$ (Fig. 1). For illustration, K_0 for CO_2 is 0.033 mol kg^{-1} atm^{-1} at a temperature of 20°C and salinity of 34.5 g kg^{-1} [11]. Hence, for a modern pCO_2 of ∼410 μatm, the equilibrium value of $[CO_2]$ in subtropical waters at the aforementioned temperature and salinity would be $0.033 \times 410 = 13.53$ μmol kg^{-1}. As for all soluble gases, the solubility (K_0) of CO_2 increases with lowering of temperature and/or salinity (Fig. 1). For CO_2, K_0 ranges from minima of 0.02–0.03 mol kg^{-1} atm^{-1} in warm tropical and subtropical regions, to 0.06–0.07 mol kg^{-1} atm^{-1} in cold polar regions [11].

Net air–sea CO_2 exchange into or out of surface sea water occurs whenever pCO_2^w is out of equilibrium with pCO_2^{atm}. When pCO_2^w is lower than pCO_2^{atm}, there will be CO_2 influx from the atmosphere into the sea water and vice versa. For example, a cooling of the water would increase K_0 and thus the water's capacity to absorb CO_2, with the opposite for a warming. However, there is a complication in that CO_2—contrary to other atmospheric gases such as O_2 and N_2—not only dissolves molecularly but also undergoes rapid dissociation reactions with water to form bicarbonate and carbonate ions (HCO_3^- and CO_3^{2-}, respectively). The following equilibria are involved: $CO_2 + H_2O \rightleftharpoons HCO_3^- + H^+ \rightleftharpoons CO_3^{2-} + 2H^+$. Note that release of H^+ lowers seawater pH because $pH = -\log_{10}[H^+]$. The sum of CO_2, HCO_3^- and CO_3^{2-} concentrations is known as Dissolved Inorganic Carbon: $DIC = [CO_2] + [HCO_3^-] + [CO_3^{2-}]$. Rather than DIC, some studies refer to this sum as ΣCO_2 (e.g. 'total CO_2') [5]. Total DIC can be measured by acidifying a seawater sample and then measuring the amount of extracted unionized CO_2 [6]; as with all concentration measurements (including salinity), DIC is sensitive to dilution/concentration associated with freshwater fluxes and is therefore often standardized to a reference salinity. There is a distinct relationship between the relative concentrations of the three so-called carbonate species (CO_2, HCO_3^- and CO_3^{2-}) and seawater pH (Fig. 2). In surface sea water, with pH between 8.0 and 8.2, HCO_3^- dominates the DIC, while CO_3^{2-} accounts for ∼10% and CO_2 for only 0.6% [11].

Another concept that is essential when discussing the ocean carbon cycle is alkalinity. A comprehensive overview of different definitions is given by Middelburg *et al.* [10]; here we consider a simplified representation. Sea water contains so-called conservative ions from strong electrolytes that are completely ionized under all conditions, and non-conservative ions from weak electrolytes that are partially ionized in relation to temperature, salinity and/or pH [11]. The most abundant conservative cations (positive ions) are Na^+, Mg^{2+}, Ca^{2+} and K^+ and the key anions (negative ions) are Cl^- and SO_4^{2-}. The charge concentrations (concentration times 1 for single-charged ions or times 2 for double-charged ions) of all conservative cations and anions add up to ∼+605.6 and −603.2 milli-mol (mmol) kg^{-1}. This indicates a charge imbalance of 2.400 mmol kg^{-1} (i.e. 2400 μmol kg^{-1}) which is known as total alkalinity (ALK_T). However, sea water is highly conductive, and cannot maintain a net charge. Therefore, the net

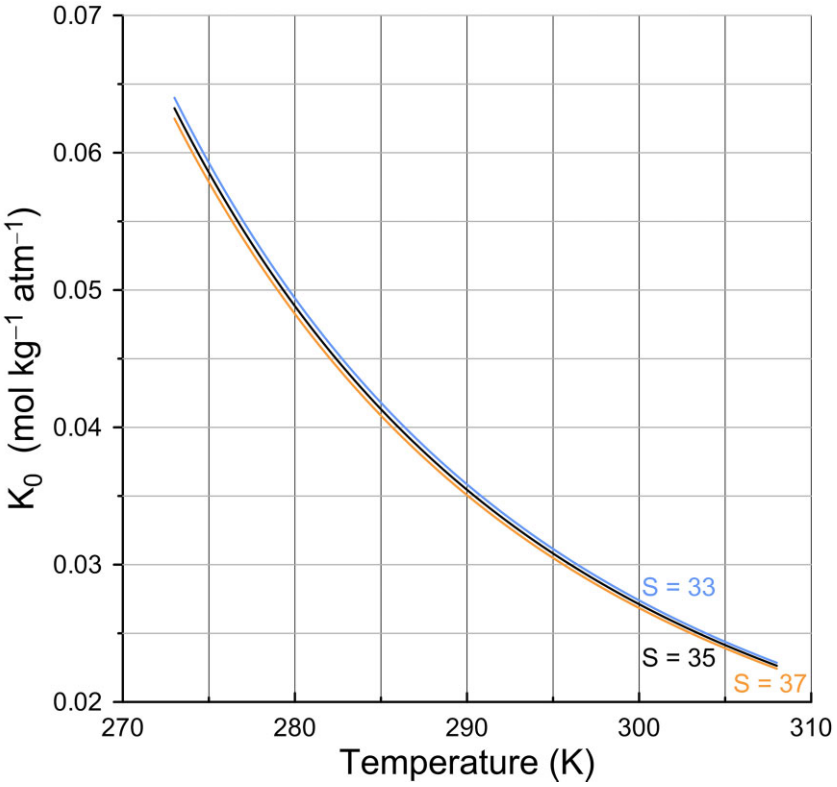

Figure 1. CO_2 solubility in sea water between 0 and 35°C, at three different salinities. After Weiss [16]. Salinity (S) was gravimetrically determined, in g kg^{-1}. As summarized in Bailey *et al.* [14], the dependence of K_0 to temperature and salinity that is commonly used in climate models (Orr et al., 2017) [15] derives from the work of Weiss [16]: $\ln(K_0) = -60.2409 + 93.4517\ (100/T) + 23.3585\ \ln(T/100) + S\ \{0.023517 - 0.023656\ (T/100) + 0.0047036\ (T/100)^2\}$, where T is temperature in Kelvin (K = °C + 273.15) and S is salinity (see also [6, 12]). Note that Bailey *et al.* [14] argue that this relationship may underestimate K_0 by up to 10% at natural salinities and sub-zero temperatures down to −2°C (polar extremes).

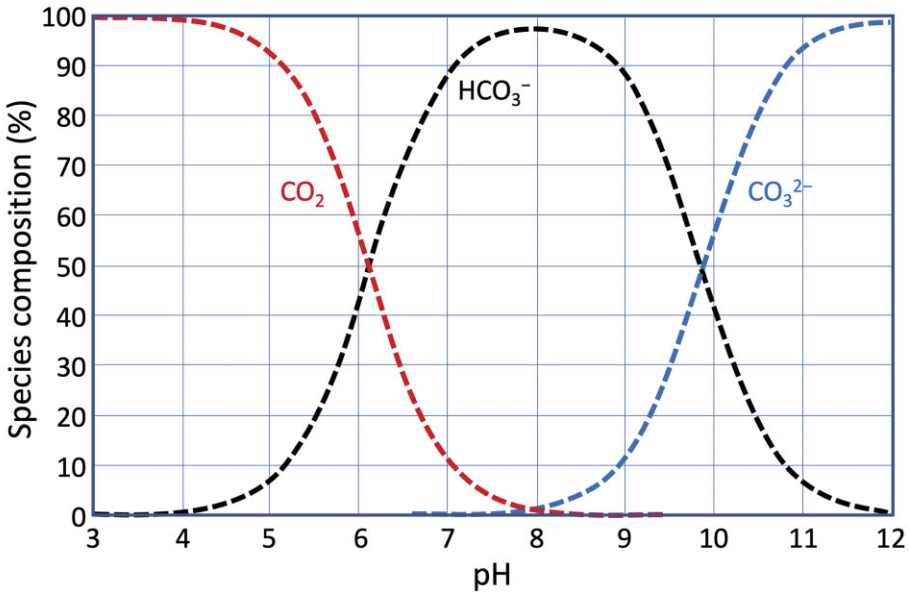

Figure 2. Bjerrum plot of carbonate species in sea water relative to pH. Here, CO_2 includes dissolved molecular CO_2 and H_2CO_3. Pre-industrial ocean pH was ~8.2, at which HCO_3^- is clearly dominant.

positive charge imbalance left by the conservative ions must be balanced by an equal-sized net negative charge imbalance due to the total non-conservative ions of −2400 µmol kg^{-1} [11, 12]. Note that this example is simplified for clarity and that more (minor) ions are involved in reality. More precisely, mean ocean alkalinity is ~2.32–2.35 mmol kg^{-1} [10, 11].

The dominant non-conservative ions are the anions HCO_3^- and CO_3^{2-}. $B(OH)_4^-$ is next, but has an ~5 times smaller charge concentration than CO_3^{2-}, and OH^- has an ~20 times smaller charge concentration still [11]. H^+ is the only non-conservative cation of note, but has a negligible charge concentration (yet, it determines pH). In other words, ALK_T is the net positive charge that must be

balanced by the dominant anions HCO_3^- and CO_3^{2-} (to be precise, $B(OH)_4^-$ should be included here too) [5], and it can be measured using some form of acidimetric titration [6]; it is independent from temperature and pressure, but sensitive (along with salinity) to dilution/concentration associated with freshwater fluxes. Given that HCO_3^- and CO_3^{2-} dominate the non-conservative ion charge concentration, the so-called carbonate alkalinity (ALK) can be described as the sum of their charge concentrations, and ALK then explains more than 95% of ALK_T [8, 11, 12]. ALK provides a useful measure of the degree to which CO_2 has reacted with water to form HCO_3^- and CO_3^{2-} [8], and it is commonly assumed that $ALK_T \approx ALK = [HCO_3^-] + 2[CO_3^{2-}]$.

Besides $ALK_T \approx ALK = [HCO_3^-] + 2[CO_3^{2-}]$, a second very useful simplification can be made, namely that $DIC \approx [HCO_3^-] + [CO_3^{2-}]$ because CO_2 contributes very little to DIC in natural sea water. Combination of these two relationships allows approximating the concentration of CO_3^{2-} from ALK_T and DIC measurements because $ALK_T - DIC \approx [CO_3^{2-}]$. Moreover, given that ALK_T is much larger than $[CO_2]$ (which equals $K_0\, pCO_2^{atm}$; see top of this section), and that $ALK_T \approx [HCO_3^-] + 2[CO_3^{2-}]$, it is evident that the charge balance of the ocean—and thus its alkalinity—creates a massive (two orders of magnitude) increase in the ocean's capacity to store carbon in the form of bicarbonate and carbonate ions, relative to a scenario without ocean alkalinity [11]. In other words, ocean alkalinity is critical to CO_2 storage in sea water. Moreover, the unique characteristic of CO_2 of reacting with water causes the total oceanic carbon concentration to be some 60 times larger than that in the atmosphere, which in turn caused the ocean to dominate atmospheric pCO_2 under natural conditions over timescales of a few millennia (a few ocean overturnings).

SPATIAL PROPERTY DISTRIBUTIONS

Williams and Follows [11] present maps of surface-water $[CO_2]$, $[HCO_3^-]$, $[CO_3^{2-}]$, DIC and ALK_T distributions. In summary, modern surface-water $[CO_2]$ varies from minima of 5–10 μmol kg^{-1} in tropical and subtropical regions, to maxima of 20–25 μmol kg^{-1} in high latitudes, especially in the Southern Ocean. The surface-water $[HCO_3^-]$ distribution is similar, varying from minima of 1600–1700 μmol kg^{-1} in tropical regions, to maxima of 2000–2100 μmol kg^{-1} in high latitudes, especially in the Southern Ocean. The surface-water $[CO_3^{2-}]$ distribution shows an opposite pattern, from minima of 100–150 μmol kg^{-1} in high latitudes, to maxima of 250–300 μmol kg^{-1} in tropical to subtropical regions. Surface-water ALK_T shows a virtually linear relationship with salinity, with minima of 2100–2250 μmol kg^{-1} in high-precipitation regions in the tropics and some high latitudes, to maxima of 2400–2500 μmol kg^{-1} in the highly evaporative centers of subtropical gyres. The surface-water DIC distribution, by definition, combines those of $[CO_2]$, $[HCO_3^-]$ and $[CO_3^{2-}]$.

The spatial ALK_T distribution is dominated by evaporation and precipitation/freshwater input, whereas the DIC distribution reflects both the influences of evaporation and precipitation/freshwater input, and changes in CO_2 solubility with temperature. There is a further complication in that full potential air–sea CO_2 exchange (equilibration) is not commonly realized—the realistic air–sea gas exchange is smaller than the potential air–sea gas exchange.

Influence of CO_2 solubility

Solubility determines the equilibrium amount of absorption for any gas, while the rate of air–sea gas transfer is affected by physical processes that include molecular diffusion, turbulent mixing, waves, bubbles and spray [11, 17]. These processes are rapid; e.g. oxygen reaches air–sea equilibrium within a month. If this were the case also for CO_2, then its air–sea exchange would keep pace with processes that tend to drive pCO_2^w away from equilibrium, creating a surface ocean with uniform pCO_2^w and a steady DIC increase with cooling from the equator to the poles [5]. However, the equilibration period for CO_2 is some 10 times longer because it involves the sizeable surface-water DIC reservoir through the reaction $H_2O + CO_2 + CO_3^{2-} \rightleftharpoons 2HCO_3^-$ (Box 1) [5, 8, 10]. The approximately 10 months needed for the DIC reservoir in the upper 50 m of surface water to equilibrate with the atmosphere is long relative to the typical surface-water residence time of a few days to years [8, 18]. In consequence, seasonal temperature may have changed since CO_2 equilibration started, and/or surface water may have traveled hundreds or thousands of kilometers into another region where local conditions are out of equilibrium. Thus, surface water pCO_2^w is forever chasing to reach equilibrium, but in most places never quite gets there (i.e. the system only reaches a so-called quasi-steady state). Surface ocean pCO_2^w overall is >80% saturated [8, 19, 20].

Spatial patterns in surface-water DIC, therefore, reflect both solubility with temperature, and superimposed deviations due to solubility changes that are more rapid than equilibration (e.g. due to seasonal temperature changes or temperature changes along flow pathways, as discussed before). But there are two more critical processes that cause superimposed deviations, namely: organic matter production and remineralization (decomposition), including upwelling of deep waters that have been enriched in carbon due to organic matter remineralization at depth; and calcium carbonate ($CaCO_3$) production and dissolution [5, 7, 8, 11, 12]. These processes relate to the so-called biological pump, by which biological processes drive important changes in oceanic carbon and alkalinity gradients. The biological pump consists of two processes: the soft tissue pump (photosynthesis/respiration) and the carbonate or alkalinity pump. These pumps are discussed in the following section.

Influence of the soft tissue and carbonate, or alkalinity, pumps

The soft tissue pump relates to the cycling of organic matter. In its most basic representation, the reaction for photosynthetic generation of organic matter (CH_2O) or—in reverse—respiration of organic matter, is $CO_2 + H_2O \rightleftharpoons CH_2O + O_2$. In this form, the relationship suggests that nutrients play no role, but this is not the case; in more detail, marine organic matter is better represented

Box 1 CO_2 exchange involves a negative (buffering) feedback. Through the buffering reaction $H_2O + CO_2 + CO_3^{2-} \rightleftharpoons 2HCO_3^-$, CO_2 added to sea water is scavenged by CO_3^{2-} ions. A minor portion of the produced HCO_3^- will then dissociate: $HCO_3^- \rightarrow H^+ + CO_3^{2-}$. This lowers the pH while, overall, there will be a net decrease in the proportion of CO_3^{2-} in DIC [12]. The result of this buffering process is that an increase of 10% in pCO_2^{atm} after full equilibration leads to a 10% increase in seawater $[CO_2]$ along with an ~1% increase in DIC; the ~1:10 ratio depends on the so-called Revelle factor (B), which scales with $DIC/[CO_3^{2-}]$ and ranges from ~8 in warm waters to ~16 in cold waters [5, 10, 11, 21]. Under warming due to anthropogenic CO_2 increase, both CO_2 solubility and—importantly—B will decrease, which makes the ocean less efficient at absorbing CO_2.

by $C_{106}H_{175}O_{42}N_{16}P_1$ or $C_{106}H_{177}O_{37}N_{16}P_1S_{0.4}$ [9], in which the involvement of the main nutrients N and P is evident. This more detailed version also reveals the C:N:P ratio of 106:16:1, which is found throughout much of the ocean and is known as the Redfield ratio, although different studies using different methods find slightly different proportions [5, 7, 8, 22–24]. So, when organic matter is formed through photosynthesis, both carbon and nutrients (N and P) are taken from sea water, while oxygen is released. Conversely, when organic matter is respired, oxygen is consumed from sea water while carbon and nutrients are released into it. Including oxygen, the C:N:P:O_2 ratio is 106:16:1:−170. Hence, the ratio of oxygen consumption for respiration relative to phosphate (PO_4^{3-}) release by that respiration is 170 to 1 [11, 25], although recent estimates suggest that this ratio may be closer to 150 or 154 to 1 [9].

Photosynthesis occurs in the sunlit upper hundred meters or so of the water column (the so-called photic layer), while respiration occurs both within the photic layer and below it (respiration of dead organic matter that sinks below the photic layer). Thus, the processes of photosynthesis, sinking and respiration of organic matter (also known as soft tissue) drive carbon and nutrients from the surface into the deep sea. This action is known as the so-called soft tissue pump. Apart from its impacts on carbon and nutrients, the soft tissue pump is a powerful agent for deep-water deoxygenation through the oxygen utilization in respiration, especially if there is limited replacement by new, oxygenated deep water.

Across all biota, the standing stock of marine biomass amounts to some 6 GtC, and about half of this concerns photosynthesizing marine primary producers [26]. This standing stock of ∼3 GtC of marine primary producers drives a global mean new primary production rate of ∼50 GtC y^{-1} [27–29], which reflects the short lifespan (high turn-over rate) of marine phytoplankton of, on average, 22 days (3/50 years). Typically, marine ecosystems are highly efficient at recycling, with high levels of remineralization of dead organic matter already within the photic layer. There is ∼11 GtC of net export production of organic matter from the photic layer, the vast majority (>90%) of which is remineralized in the water column at depth (it becomes DIC—and most of the remineralization happens within the upper 1000 m of the water column), while considerable remineralization also happens at the sea floor and in the sediments. On average, only ∼0.2 GtC of organic matter (as particulate organic carbon) gets preserved in seafloor sediments [27–30]; i.e. less than 0.1% of the initial production (Fig. 3). More than 80% of this burial occurs in coastal and ocean margin sediments, with deep sea burial estimated at <0.01 GtC [33], so that water depth appears to be a critical controlling factor for organic carbon burial potential. The soft-tissue pump causes a major reduction in surface-water DIC and pCO_2^w through photosynthesis, and raises DIC and pCO_2^w at depth through respiration (Fig. 3). It also causes a minor increase in ALK_T of surface waters and minor decrease in ALK_T at depth because of uptake and release of nutrients (e.g. [5, 56]).

The carbonate or alkalinity pump relates to the processes involved in hard ($CaCO_3$) body part formation and dissolution. In its most basic form, the reaction involved in the formation and dissolution of $CaCO_3$ is: $Ca^{2+} + CO_3^{2-} \rightleftharpoons CaCO_3$, but it is often represented in relation to the much more common bicarbonate ion: $Ca^{2+} + 2HCO_3^- \rightleftharpoons CaCO_3 + H_2O + CO_2$. The latter might seem to suggest that 1 mol of CO_2 is produced for every 1 mol of $CaCO_3$ production, but this is misleading because most of the liberated CO_2 immediately reacts with water following the equilibrium reactions $CO_2 + H_2O \rightleftharpoons HCO_3^- + H^+ \rightleftharpoons CO_3^{2-} + 2H^+$ (Box 2), so that the actual CO_2 increase is in the range of 0.6–0.8 depending on pH/pCO_2 of the water [12, 36]. The amount of $CaCO_3$ permanently deposited on the ocean floor is determined by the flux of calcium into the ocean from rivers [7] and occurs mainly through formation of $CaCO_3$ tests of marine organisms, especially planktic foraminifera and calcareous nannoplankton [37] and to a lesser extent coral reefs and inorganic precipitates [38, 39]. The $CaCO_3$-bound carbon is referred to as particulate inorganic carbon (PIC). Rivers were thought to bring ∼0.2 GtC y^{-1} of PIC into the ocean (although recent estimates indicate that this number may be some 7 times smaller [40] and ∼1 GtC y^{-1} of PIC is formed in the surface ocean. About 0.3 GtC y^{-1} of PIC is buried as $CaCO_3$ in shallow-water sediments. Some 0.9 GtC y^{-1} of PIC is exported (sinks) to below the photic zone (∼80%) [7, 37, 41, 42], of which 0.8 GtC y^{-1} is dissolved into deeper waters (it becomes DIC—about half of this dissolution happens in the upper 1–2 km of the water column), and only ∼0.1 GtC y^{-1} is buried into deep-sea sediments (Fig. 3) [27–30]. $CaCO_3$ formation reduces ALK_T and DIC and somewhat raises pCO_2^w in surface waters, while dissolution of $CaCO_3$ at depth increases ALK_T and DIC and somewhat lowers pCO_2^w in deep water (Box 2 and Fig. 4).

VERTICAL GRADIENTS—CARBON TRANSPORT INTO THE OCEAN INTERIOR

For vertical gradients, the 'pumps' discussed in Section 'Influence of the soft tissue and carbonate, or alkalinity, pumps' are of critical importance. Overall, some 4–5 times more carbon is exported from the photic layer by the soft tissue pump (st) than by the carbonate pump (carb). This proportionality is represented by the so-called rain ratio (C_{st}/C_{carb} = 4:1 to 5:1) [5, 8, 11, 12, 43, 44]. As a consequence, the soft tissue pump dominates vertical DIC gradients in the ocean. Because the soft tissue pump involves also PO_4^{3-} (in Redfield ratio relative to carbon), while the carbonate pump does not affect PO_4^{3-}, the contributions of the soft tissue and carbonate pumps to measured vertical DIC gradients can be disentangled using measured vertical PO_4^{3-} gradients. Conversely, the contributions of the carbonate pump can be approximated using the ALK_T distribution (Fig. 4) [8, 35]. It is critical to emphasize that use of the PO_4^{3-}(phosphate)-based estimate for the soft tissue pump and the ALK_T-based estimate for the carbonate pump yields DIC changes that would result from these pumps if there were no concomitant air–sea gas exchange working to 'reset' the carbon equilibrium. Notably, air–sea gas exchange, in combination with ocean circulation, would over time allow some of the accumulating deep CO_2 to outgas back into the atmosphere. Hence, real vertical DIC changes are expected to differ somewhat from the sum of the P-based estimate for the soft tissue pump and the ALK_T-based estimate for the carbonate pump [8]. In fact, combining these two estimates reveals that the soft tissue pump (ΔC_{st}) can explain at most 220 μmol kg^{-1}, or 70%, of the observed vertical DIC gradient (ΔDIC) of ∼315 μmol kg^{-1} of pre-industrial times (before anthropogenic CO_2 emissions), and the carbonate pump (ΔC_{carb}) at most 60 μmol kg^{-1}, or 20% [8]. The residual effect of ∼35 μmol kg^{-1}, or 10% of ΔDIC, relates to the net effect of the so-called gas-exchange pump [8] (Box 3 and Fig. 5). To understand why the net gas-exchange effect is positive, a bit more detail is needed.

Combination of the net biological (bio) and gas-exchange (gasx) pumps determines the relationship that drives ΔDIC, according to $\Delta DIC = \Delta C_{bio} + \Delta C_{gasx}$. We have seen above that ΔC_{bio} splits into the soft tissue (st) and carbonate (carb) pumps, so that $\Delta DIC = \Delta C_{st} + \Delta C_{carb} + \Delta C_{gasx}$. The gas-exchange pump in turn can

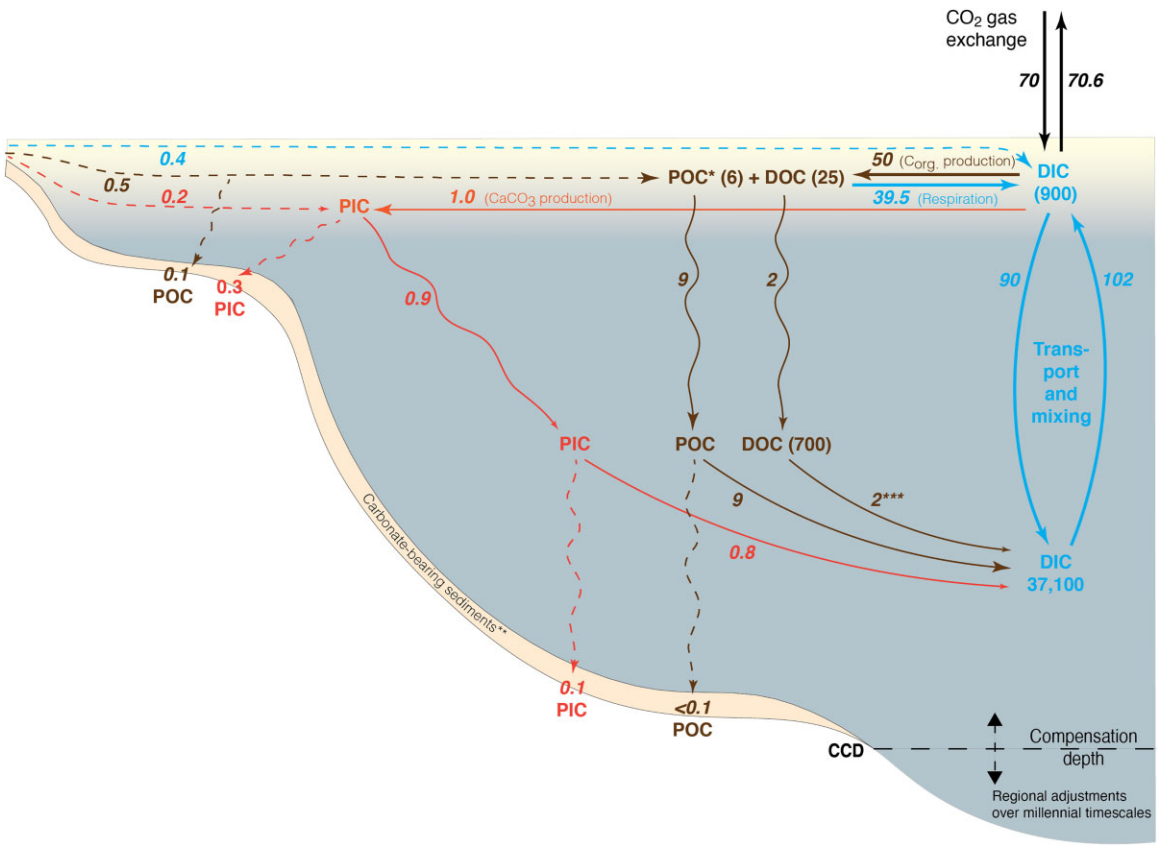

Figure 3. Pre-industrial flow of carbon through the ocean system. Pathways, reservoir sizes (regular font, in GtC) and fluxes (italic numbers, in GtC y^{-1}) are indicated with different colors for: PIC (red), dissolved inorganic carbon (DIC; blue) and particulate and dissolved organic carbon (POC and DOC; brown). DOC is the organic matter that can fit through a filter, while POC is the organic matter that is too large and thus is filtered out (common filter sizes between 0.7 and 0.22 μm). Basis diagram after Sabine and Feely [29]. *, Marine biota total biomass value of 6 GtC after Bar On *et al.* [26]; **, surface sediment total 150 GtC [26, 27, 29] and 1600 GtC [11, 34] and ***, exponential decrease with depth due to respiration [32].

Box 2. Somewhat counterintuitively, surface-water production of $CaCO_3$ does not reduce surface-water pCO_2^w, but instead increases it. This is because CO_3^{2-} is consumed in the reaction $Ca^{2+} + CO_3^{2-} \rightarrow CaCO_3$. The CO_3^{2-} reduction leads to partial compensation for this loss via a shift in the buffering reaction $2HCO_3^- \rightleftharpoons H_2O + CO_2 + CO_3^{2-}$ (here reorganized to indicate the direction of shift from left to right), which implies a release of CO_2 and thus an increase in surface-water pCO_2^w. The CO_2 release can also be viewed from the fact that $CaCO_3$ formation reduces surface-water ALK_T by twice as much as DIC because of the double charge of Ca^{2+} versus the single C atom used, so that the $CaCO_3$ arrow crosses pCO_2^w contours to higher values (Fig. 4). The opposite applies to carbonate dissolution, which drives a reduction in pCO_2^w [5].

also be split into two components. One is temperature dominated, with a small influence of freshwater fluxes [8, 45], and reflects the physical transfer of cold, carbon-rich water from the surface at high latitudes into the deep sea; this is known as the solubility pump (or thermal gas-exchange pump; $\Delta C_{gasx(sol)}$), which enhances DIC at depth [8, 11, 46]. The second component of the gas-exchange pump is driven by surface carbon chemistry changes that result from biological processes; this is the biological gas-exchange component ($\Delta C_{gasx(bio)}$) [8]. Note that the latter is not technically a 'pump' in that it does not act against a gradient. Instead, it concerns the respiration driver behind high DIC and pCO_2^w values at depth that, upon upwelling, fuel outgassing into the atmosphere. Thus, the complete relationship becomes: $\Delta DIC = \Delta C_{st} + \Delta C_{carb} + \Delta C_{gasx(sol)} + \Delta C_{gasx(bio)}$ (Fig. 5). Because $\Delta C_{gasx(bio)}$ represents the gas-exchange-related 'dampening' of DIC gradients relative to the potential PO_4^{3-}-based estimates of ΔC_{bio}, values for $\Delta C_{gasx(bio)}$ are negative. In other words, the two gas-exchange terms ($\Delta C_{gasx(sol)}$ and $\Delta C_{gasx(bio)}$) have opposing influences. The net gas-exchange pump influence is only about a third of what would be expected based on thermal gas-exchange arguments alone (Box 3) [8].Because the soft tissue pump and carbonate pump have different impacts on ALK_T, DIC and pCO_2^w, the net effect of the total biological pump on both surface-water and deep-water chemistry over time depends on the rain rate of organic carbon to $CaCO_3$-bound carbon [5, 8, 11, 12]. Other plankton groups, notably diatoms and radiolaria, build their hard body parts out of opal (SiO_2), and yet others are organic-walled (e.g. dinoflagellates). These groups affect only the soft tissue pump; they do not contribute to the carbonate pump. Hence, when considering processes that utilize marine primary production and the biological pump to enhance CO_2 removal from the atmosphere into the ocean, diatoms are of particular interest because they completely lack the carbonate pump, but even the dominant carbonate-bearing coccolithophores remain of interest because their soft tissue pump component outperforms their carbonate pump component. Moreover, the presence of mineral (especially carbonate) hard body parts provides ballasting of organic carbon, which increases biological pump efficiency [48, 49].

Box 3. The solubility or thermal gas-exchange pump ($\Delta C_{gasx(sol)}$) is affected by the (slow) surface water pCO_2^w equilibration discussed above and its interaction with the large-scale oceanic surface-to-deep water circulation. For an average surface-to-deep water cooling of 18°C and a DIC solubility change of 9 μmol kg^{-1} $°C^{-1}$ [47], $\Delta C_{gasx(sol)}$ would be expected to contribute ∼155 μmol kg^{-1} to ΔDIC, if pCO_2^w equilibration were instantaneous [8]. The slowness of the realistic air-sea pCO_2^w equilibration, discussed above, reduces the expected $\Delta C_{gasx(sol)}$ contribution to ∼100 μmol kg^{-1} [8, 45]. This is still some 3 times greater than the net ΔC_{gasx} contribution to ΔDIC (∼35 μmol kg^{-1}). The discrepancy arises from the impact of the second component of the gas-exchange pump ($\Delta C_{gasx(bio)}$), and its impact can therefore be estimated as $\Delta C_{gasx(bio)} = \Delta C_{gasx} - \Delta C_{gasx(sol)} = 35 - 100 = -65$ μmol kg^{-1} (Fig. 5). The potential effect of the biological pump on vertical DIC gradients was determined by $\Delta C_{bio} = \Delta C_{st} + \Delta C_{carb} = 220 + 60 = 280$ μmol kg^{-1}. Now, we see that biology-related gas exchange moderates that value to a realistic net value of $\sim 280 - 65 = 215$ μmol kg^{-1}. The biology-related gas-exchange component ($\Delta C_{gasx(bio)} = -65$ μmol kg^{-1}) appears to offset two-thirds of the solubility-related gas-exchange component ($\Delta C_{gasx(sol)} = 100$ μmol kg^{-1}). Hence, simple solubility-based arguments about carbon storage in the interior of the ocean may produce overestimates by a factor of 3. And if the simple solubility arguments fail to account for slowness of the realistic air-sea pCO_2^w equilibration, then this overestimation rises to a factor of 5.

USING OCEAN BIOGEOCHEMISTRY TO MITIGATE CO_2 EMISSIONS

Carbon storage mechanisms

Broecker and Peng [5] argue that simple physical solution would have resulted in ocean uptake of only ∼3% of humanity's CO_2 emissions since the onset of the industrial revolution (almost all of the emissions would have remained in the atmosphere). However, early estimates suggested that the ocean has instead taken up ∼40% of humanity's historical CO_2 emissions [50], while the uptake fraction of current emissions is 23 ± 5% (measured for 2009–18) [5, 51]. Broecker and Peng [5] also state that the only two pathways for significant amounts of CO_2 to enter into the oceanic DIC reservoir are the buffering reaction ($H_2O + CO_2 + CO_3^{2-} \rightleftharpoons 2HCO_3^-$) that affects CO_2 entering surface waters via air–sea exchange and deeper water via organic matter remineralization, and the $CaCO_3$ dissolution reaction ($CaCO_3 + H_2O + CO_2 \rightleftharpoons Ca^{2+} + 2HCO_3^-$). The CO_3^{2-} in the first equation is that dissolved in the ocean, and the $CaCO_3$ in the second equation is entirely dominated by the massive mass of interchangeable carbonate in marine surface sediments, which is estimated between 150 GtC (1250 $GtCaCO_3$) [27, 28, 30] and 1600 GtC (13 330 $GtCaCO_3$) [34, 11] (Fig. 3).

$CaCO_3$ dissolution is determined by the so-called saturation state of sea water (**Ω**), which is a function of the carbonate ion concentration; $[CO_3^{2-}]$ [5, 12]. If we assume that $[Ca^{2+}]$ is more or less uniform and constant in the ocean, then the saturation state of seawater is given by: $\mathbf{\Omega} = [CO_3^{2-}]/[CO_3^{2-}]_{sat}$, where $[CO_3^{2-}]$ is the actual concentration in a seawater sample, and the subscript sat indicates saturation at the pressure, temperature and salinity of the sample. $CaCO_3$ tends to grow under supersaturated conditions ($\mathbf{\Omega} > 1$), and to dissolve under undersaturated conditions ($\mathbf{\Omega} < 1$). Because $[CO_3^{2-}]_{sat}$ is a weak function of temperature and salinity but a strong function of water depth (pressure), deeper waters are more corrosive to $CaCO_3$ than shallower waters [52, 53]. In essence, $CaCO_3$ becomes more soluble with lowering temperatures, and especially with increasing pressure (depth). At typical deep-sea temperatures (∼2°C), $CaCO_3$ is about twice as soluble at 500 atmospheres (atm) of pressure (=∼5000 m depth) as at 1 atm of pressure (surface) [5]. An approximate relationship relative to pressure only is $[CO_3^{2-}]_{sat} \approx (4.35 \times 10^{-7}/[Ca^{2+}])\ e^{(P/511)}$ [53], where P is water pressure at the depth evaluated and $[Ca^{2+}]$ is almost constant at $\sim 10.2 \times 10^{-3}$ mol kg^{-1} [54], so that the relationship further simplifies to $[CO_3^{2-}]_{sat} \approx 4.27 \times 10^{-5}\ e^{(P/511)}$. The seawater saturation state (**Ω**) contrasts the actual $[CO_3^{2-}]$ with the saturation value $[CO_3^{2-}]_{sat}$, and it is especially the biological pump that causes fluctuations in $[CO_3^{2-}]$. Its combined soft-tissue and carbonate processes lead to a strong increase in DIC and a considerable increase in ALK_T (Box 4 and Fig. 6), which drive a rapid decrease in $[CO_3^{2-}]$ and, hence, reduce **Ω**. This makes deep water that has received more mineralization products more

Box 4. To illustrate the impacts of soft tissue remineralization and carbonate dissolution on seawater $[CO_3^{2-}]$, an example is borrowed from Broecker and Peng [5]. Both soft tissue remineralization and carbonate dissolution increase DIC; in more detail, the soft tissue remineralization maximum resides shallower than the carbonate dissolution maximum, but this is ignored here. However, the effects of nitrate (NO_3^-) in the soft tissue pump (NO_3^-) need to be included (Fig. 6). For every 1 mol of C in soft tissue, some 0.15 moles of NO_3^- are included (see Redfield ratio). For a molar rain rate of 4:1 for carbonate-producing plankton, remineralization at depth releases $4 \times 0.15 = 0.6$ moles of NO_3^- (a change in charge concentration of −0.6 moles in deep-water ALK_T). Hence, combined remineralization and dissolution increase deep-water DIC ≈ $[HCO_3^-] + [CO_3^{2-}]$ by 5 moles. Meanwhile, deep-water ALK_T increases by +2 (release of 1 mole of Ca^{2+}) and −0.6 moles (due to NO_3^- release) = 1.4 moles in total. There are many additional influences, which will be ignored here for clarity [10]. The change in ALK_T, therefore, is 28% of the change in DIC. Starting with a water mass with DIC = 2000 μmol kg^{-1} and ALK_T = 2200 μmol kg^{-1}, and assuming that this water parcel would undergo a total DIC change of 200 μmol kg^{-1} due to remineralization and dissolution (to 2200 μmol kg^{-1}), then this water parcel would have undergone a $(1.4/5) \times 200 = 60$ μmol kg^{-1} increase in ALK_T (to 2260 μmol kg^{-1}). Given the relationship between $[CO_3^{2-}]$, ALK_T and DIC discussed previously, $[CO_3^{2-}] \approx ALK_T - DIC = 2200 - 2000 = 200$ μmol kg^{-1} in the original water parcel, while $[CO_3^{2-}] \approx ALK_T - DIC = 2260 - 2200 = 60$ μmol kg^{-1} in the modified water parcel. Hence, $[CO_3^{2-}]$ has dropped greatly due to the combined effect of remineralization and dissolution, reducing **Ω** and making deep water more corrosive to $CaCO_3$. Meanwhile, given the simplification DIC ≈ $[HCO_3^-] + [CO_3^{2-}]$ discussed previously, original $[HCO_3^-]$ was 2000 − 200 = 1800 μmol kg^{-1}, while the modified-water $[HCO_3^-]$ is 2200 − 60 = 2140 μmol kg^{-1}; i.e. $[HCO_3^-]$ has gone up by 340 μmol kg^{-1}. This is because the CO_2 released from mineralization of soft tissue exceeds the amount of CO_3^{2-} released by dissolution of carbonate, and the buffering reaction ($H_2O + CO_2 + CO_3^{2-} \rightleftharpoons 2HCO_3^-$) combines the excess released CO_2 with CO_3^{2-} that was in the water already, producing HCO_3^-.

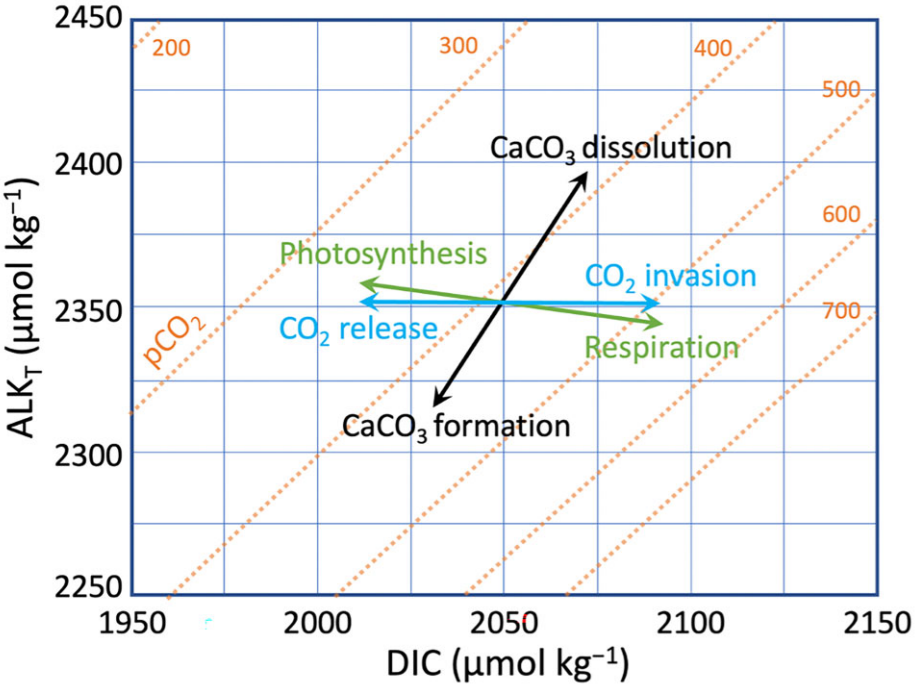

Figure 4. Effect of key processes on pCO_2 in ALK_T–DIC space. Seawater pCO_2 (orange lines and numbers, in μatm) is calculated at a temperature of 25°C, salinity of 35 and pressure of 1 atm (water depth of 0 m). $CaCO_3$ dissolution increases seawater ALK_T and DIC in a ratio of 2:1, with a net effect of decreasing seawater pCO_2. $CaCO_3$ formation has the opposite effects. CO_2 invasion and release into/from the ocean only affects seawater DIC. Photosynthesis mainly consumes seawater DIC and only slightly increases seawater ALK_T due to nutrient uptake; respiration has the reverse effect. Modified after Yu *et al.* [35].

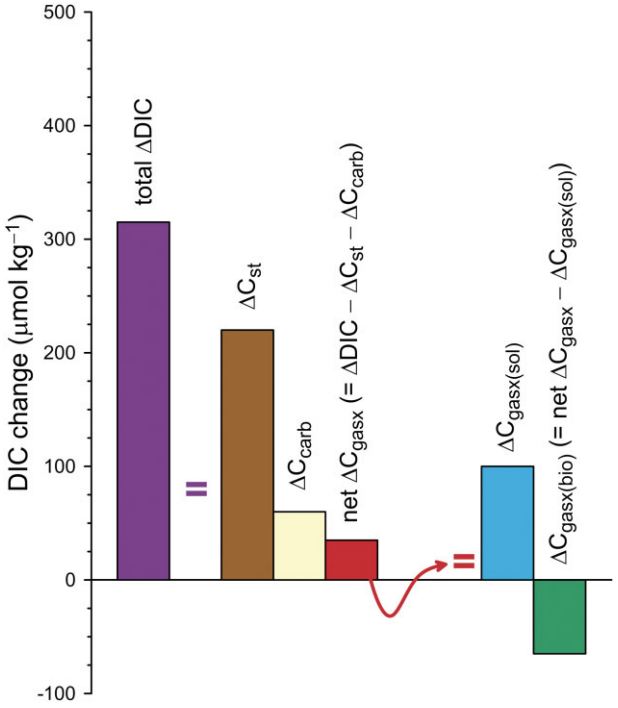

Figure 5. Total vertical DIC gradient and its component parts. The total vertical DIC gradient (purple) comprises the soft tissue (brown), carbonate/alkalinity (cream) and net gas exchange (red) contributions. The net gas exchange contribution (red) results from a solution component (blue) and a biological component (green).

corrosive to $CaCO_3$ (Box 4). As a result, $CaCO_3$ can exist in marine sediments only down to a certain depth, and is absent below that level because of dissolution (below). Given that presence of $CaCO_3$ makes marine sediments pale beige or gray in color, and that its absence leaves dark brown-gray colors (clay minerals), one can imagine a sort of 'snow line' with $CaCO_3$ present above it, but not below it [55].

Several important levels have been identified with regard to carbonate dissolution in the ocean. The shallowest marks the depth below which notable $CaCO_3$ dissolution occurs (it is often referred to as the lysocline, although this term is through the literature used for a variety of slightly different, related concepts). Considering seafloor sediments, this level is commonly recognized at a depth where overlying water is still supersaturated ($\Omega > 1$); the observed carbonate dissolution is driven by saturation reduction due to respiration within sediment pore waters (e.g. [31]). The next level down is the saturation horizon, where ocean water itself first becomes undersaturated ($\Omega = 1$). Note that the discussion here focuses entirely on calcite and ignores the metastable form aragonite(e.g. [5, 12]). Roughly a kilometer below the saturation horizon lies the compensation depth, which geochemically is the level where dissolution at the sediment–water interface exactly balances the rain of $CaCO_3$ from above [53, 57–59], and which geologically is the level where the sedimentary $CaCO_3$ content drops to ~10% due to dissolution [53, 60–62]. Finally, the so-called snow line is recognized, below which no solid calcite is found in the sediment due to dissolution [53, 55].

The compensation depth and the snow line are identical when the system is in steady state. However, when a large CO_2 perturbation makes its way into the ocean interior (e.g. the anthropogenic emissions signal), the saturation horizon and geochemical compensation depth shift to shallower water, and the $CaCO_3$ that had accumulated above the snowline now falls below the compensation depth, causing intense dissolution. This so-called carbonate compensation process is the ultimate natural mechanism

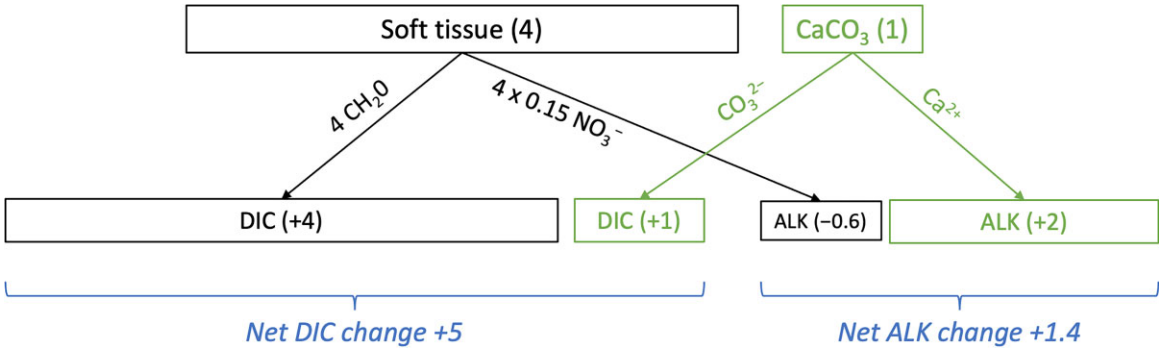

Figure 6. Schematic impacts of the soft-tissue (black) and carbonate/alkalinity (green) pumps on deep-water DIC and ALK_T. Values in molar units. The example considers the influences of soft (organic) tissue and carbonate formed in the upper water column that sink with an assumed rain ratio of 4:1, and then remineralize and dissolve in deeper waters. Following an example presented in Broecker and Peng [5].

for 'cleaning up' a major CO_2 perturbation [11, 34]. It requires the large-scale ocean circulation (transporting the CO_2) to make many passes through the deep sea where the $CaCO_3$ lies; each pass takes many centuries to a millennium, and during each pass only a fraction of the ocean volume interacts with the sedimentary $CaCO_3$ [5]. Hence, carbonate compensation is an intrinsically slow process. Over many tens of thousands of years, the CO_2 anomaly gets smaller and smaller following an exponentially decaying curve, and eventually only up to ∼10% of the original emissions spike remains in the atmosphere [11, 34, 63–65]. In specific locations in the deep western North Atlantic, enough anthropogenic CO_2 has now been transported into the deep sea via North Atlantic Deep Water formation to have started the process of carbonate compensation (the calcite compensation depth has risen ∼300 m) [66].

Given that there is no conceivable way of accelerating carbonate compensation to timescales short enough to be of relevance to society, oceanic methods for anthropogenic CO_2 capture instead need to consider shorter-term processes. This means storage of the sequestered carbon (i) in the vast oceanic DIC reservoir with multi-centennial timescales and/or (ii) through burial in sea-floor sediments with timescales up to millions of years. To achieve this, methods have been proposed that manipulate either the soft tissue pump, or ocean alkalinity.

Using the soft-tissue pump

The soft tissue pump is responsible for the majority of carbon transport from the ocean surface into the ocean interior, and even into sea-floor sediments (Fig. 3). It involves the reaction $CO_2 + H_2O \rightleftharpoons CH_2O + O_2$, with the understanding that carbon changes go hand-in-hand with similar-sign changes in N and P, and opposite-sign changes in O_2, following ratios of approximately $C{:}N{:}P{:}O_2 = 106{:}16{:}1{:}-170$ [11, 25]; although recent estimates for the O_2:P and O_2:C ratios suggest −150 to −154 and ∼−1.45, respectively [9]. Thus, the soft tissue pump brings not only C into deeper waters, but also the major (or macro-) nutrients P and N. Upwelling of waters enriched in these elements back into the photic layer will trigger new production, consuming C, N and P in roughly similar proportions as they occur in the water. However, not only P and N are important, but also trace amounts of other elements following the extended Redfield ratio: $C_{124,000}\ N_{16,000}\ P_{1,000}\ S_{1,300}\ K_{1,700}\ Mg_{560}\ Ca_{500}\ Sr_5\ Fe_{7.5}\ Zn_{0.8}\ Cu_{0.38}\ Co_{0.19}\ Cd_{0.21}\ Mo_{0.03}$ [67, 68]. In some oceanic regions, high macro-nutrient conditions exist but productivity remains low (i.e. concentrations of chlorophyll, the main compound involved in photosynthesis, remain low); these are known as high nutrient low chlorophyll (HNLC) regions, and productivity in these regions is often limited by a shortage of iron in a bio-available form (e.g. [69–75] and references therein). Biological production in ∼30% of the modern surface ocean is thought to be limited primarily by Fe [68, 76]. Upwelling in a HNLC region leads to CO_2 outgassing because of a lack of new biological production to consume the carbon that accumulated in the water through remineralization; thus $pCO_2^w > pCO_2^{atm}$. In consequence, there is considerable interest in 'fertilizing' such areas (notably the Southern Ocean, Equatorial Pacific and North Pacific) with iron to stimulate biological productivity and thus reduce pCO_2^w, which in turn would minimize outgassing and possibly even achieve net CO_2 sequestration—the scale of the net CO_2 impact remains debated [74–75]. Due to uptake of the nutrients NO_3^- and PO_4^{3-}, enhanced photosynthesis also leads to an increase in surface-water alkalinity (Fig. 4), which promotes further CO_2 uptake (see also next section). For such fertilizing approaches to be successful, a means needs to be found to make newly produced POC sink rapidly into the deep sea (preferably to the sea floor), to avoid immediate reversal of the process by remineralization in shallow water (Box 5). However, several issues need to be considered; notably oxygen utilization and nutrient robbing, as discussed next.Respiration of sinking organic matter utilizes oxygen, both in the water column while the organic matter is sinking, and on/in the sea floor once organic matter has accumulated there. Even if burial of a larger than normal proportion of organic matter in sediments could somehow be achieved, the fraction buried will still be only a minor portion of the total export production; the vast majority of sinking organic matter will be respired in the water column (as mentioned, water depth thus exerts an important control on burial rates), and both on the sea floor and at shallow burial depths inside the sediments. For example, ∼3–5% of gross primary production ends up on the seafloor today and only a tenth to a fifth of this is preserved in sediments while the rest is remineralized within the sediments through further oxidation using oxygen and then sulfate ($2CH_2O + SO_4^{2-} \rightarrow 2HCO_3^- + H_2S$) and subsequent microbial methanogenesis ($2CH_2O \rightarrow CO_2 + CH_4$) [9, 77]. Even in modern regions of optimum net organic carbon burial fluxes, burial represents only ∼1% of primary production [78]. A region's existing type of ecosystem plays an important role; ecosystems with high nutrient retention and a super-efficient microbial loop (notably, in warm water, which accelerates respiration rates; e.g. the Red Sea) have much lower proportions of carbon burial relative to new production than other, less efficiently recycling ecosystems [79].

Modeling of future warm (high CO_2) conditions with doubled phosphorus and iron input indicates that organic carbon burial in marine sediments might eventually draw down a total of

Box 5. It is possible that marine biomass stocks, including those potentially interesting to fisheries, might increase in a fertilized region. However—even ignoring that this growth may be (partially) offset by a decline in downstream regions—such growth would be a one-time change only, followed by a new steady state where flux in equals flux out. Even if a doubling or tripling of the ∼3 GtC global biomass stock in classes larger than single-celled plankton [26] could be achieved, such a one-time change would only represent a few percent of the oceanic C sequestration desired. Hence, the bulk of productivity-based oceanic C sequestration must be done by action of the soft-tissue pump, with focus on the rapidly overturning single-celled phytoplankton, rather than by a marine biomass stock expansion at higher trophic levels (but note that there are also proposals for artificial upwelling as a method for carbon removal that focuses on multi-cellular macro-algae; e.g. *Sargassum*).

∼1600 GtC, although this would take tens of thousands of years, and will be associated with massive spatial expansion of anoxic deep-water conditions, similar to that during two major oceanic anoxic events in Earth's history [80]. However, ∼1600 GtC greatly exceeds what may be needed to limit global warming to 1.5°C above pre-industrial levels, which instead requires 70–280 GtC removal by 2100 [81]. Land-based CO_2 removal of ∼100 GtC may be conceivable with large-scale reforestation and soil regeneration (especially when including soil biochar enrichment) and technological solutions may increase this ([4, 82–85] and references therein). Hence, a similar marine contribution of ∼100 GtC would be a useful target, which would avoid the worst of the side-effects of the ∼1600 GtC model of Ruvalcaba Baroni *et al.* [80]. For example, model experiments by Oschlies *et al.* [86] considered ∼70 GtC over a 100-year period.

The key challenge for ocean iron fertilization methods is to devise effective ways of transporting organic matter to the sea floor (which is especially difficult in deep waters) and achieve burial with as little remineralization as possible, to avoid complications such as seawater de-oxygenation [75, 86–89] and substantial downstream return-flow of CO_2 from sea water (see Oschlies *et al.* [86] for the Southern Ocean and Gnanadesikan *et al.* [90] for the tropical Pacific). Ref. [75] reviewed all major iron fertilization experiments to date, and concluded that '… detection of significant carbon export below the winter mixed layer following an [iron-triggered] increase in primary productivity required at least three conditions: (1) a shift to a diatom-dominated community; (2) low bacterial respiration and grazing-pressure rates within the mixed layer and (3) a sufficient experimental duration [to allow observation of] both immediate and delayed responses to iron addition'. Possibilities for artificially accelerating organic-matter transport to the sea floor include ballasting of phytoplankton blooms with clay minerals or other detrital (e.g. dust) material [48, 91–94, 134], and/or specifically triggering phytoplankton blooms in regions where the physical circulation assists excess DIC transport into the deep sea, such as the Ross Sea near Antarctica [95]. The latter condition may more broadly apply to the region around Antarctica to the south of the so-called Southern Ocean Biogeochemical Divide, where circulation accumulates macro-nutrients that can sustain major productivity increases, and where rapid sinking of waters assists excess DIC transport from the surface into the deep sea [96].Achieving rapid sinking and burial of organic matter in fertilized HNLC regions has negative side-effects as well; the associated nutrient export from surface waters and their accumulation at and above the sea floor represent significant changes in the long-standing ecosystem operation of these regions, with repercussions throughout their food webs. Moreover, nutrient deprivation in areas downstream of the fertilized HNLC regions, a process called nutrient-robbing (e.g. [69, 86, 100–102]), is also likely to have adverse impacts on ecosystem operation (see also Box 6). Finally, cessation of iron fertilization in many locations appears to result in a 'rebound' effect of net CO_2 outgassing that has a major negative impact on the efficiency of iron fertilization [95]. The wide range of ecosystem impacts of iron fertilization must be much better understood before large-scale implementation of the method is contemplated because they include potentially disastrous (i) marine feedbacks that partly or entirely offset the CO_2 sequestration gains in the fertilized HNLC region, including production of the powerful greenhouse gases N_2O or methane, and a rebound effect when iron fertilization is stopped, which would quickly erode the net benefit (and cost efficiency) of iron fertilization (e.g. [74, 75, 86, 87, 90, 95, 103]); (ii) toxic algal bloom development [75, 104, 105]; (iii) water-column de-oxygenation [75, 86–89] and/or (iv) side-effects to critical ecosystem services over a much wider spatial domain [69, 74, 97] (Box 6).

Box 6. Recent work on iron transport and limitation further emphasizes concerns that nutrient-robbing associated with fertilizing HNLC regions may affect nutrient cycling and ecosystem interdependences on a global scale, and casts doubt over the net CO_2 sequestration potential of iron fertilization. It proposes that, over geological time, a global macronutrient and micronutrient colimitation with optimized net productivity may have developed in the oceans, which is mediated by macronutrient, iron, and ligand redistribution via ocean circulation; the so-called ligand-iron-microbe feedback [69]. Ligands are phytoplankton- and other microbe-produced 'organic molecules that bind to iron and act as a refuge from loss by scavenging and precipitation, and […] most oceanic dissolved [bio-available] iron is associated with organic chelating ligands' [69]. The authors propose that ligands produced by phytoplankton using nutrients in the dust-replete North Atlantic, which is (via Antarctic Intermediate Water) downstream of the Southern Ocean HNLC region, cause iron transport via deep currents back into the Southern Ocean, where it feeds phytoplankton. This feedback keeps iron available in the ocean in 'just enough' amounts. Following this framework, further iron additions to the Southern Ocean are unlikely to drive appreciable increases in net global productivity (thus, CO_2 sequestration) on a global scale, although major detrimental ecosystem impacts may be caused [69, 97]. Yet, the framework represents a highly idealized representation of the complex iron cycle in the ocean [68], which casts doubt on its inferred perfectly closed loop. Moreover, ocean carbon inventory changes in the geological past in part reflect an important contribution of iron fertilization in ocean C sequestration (e.g. [98, 99]), which challenges the conclusion of Lauderdale *et al.* [69] that iron additions would not appreciably affect CO_2 sequestration.

All this should not be taken to mean that ocean iron fertilization should be discarded as a potential method for atmospheric carbon removal. Instead, it emphasizes that careful work is needed to better understand the true scale of the benefits, and the likelihood of side-effects that might potentially offset any benefits. There are not enough data to fully assess what exactly might be expected from ocean iron fertilization. Because of the potentially wide-ranging impacts, a targeted research effort is needed to resolve the governing framework of processes and interactions before large-scale implementation is sought.

Altering ocean alkalinity

Theoretically, there is vast potential for CO_2 sequestration into the interior of the ocean via ocean alkalinity enhancement (OAE) (e.g. [4, 88, 106–109]). This leads to storage in the oceanic DIC reservoir, over multi-decadal to multi-centennial timescales. The method essentially works by artificially increasing the positive charge concentration of cations in sea water, with specific interest in Ca^{2+} and Mg^{2+}. This increase would be realized through addition of ground silicate rock or industrially produced lime (Box 7) to coasts in warm regions where wave agitation keeps mobilizing and pulverizing the material and high temperatures maximize weathering rates, or to open-ocean surface waters (e.g. [106, 109], and references therein). Note that the direct CO_2 consumption during chemical weathering in this method is strongly augmented by indirect CO_2 drawdown associated with the method's alkalinity addition to the ocean (see below).The mining effort needed to obtain sufficient silicate rock and/or limestone (for lime production) for removal of several gigatons of CO_2 per year is similar to the mining effort for the current global cement industry (~7 Gt of source rock per year [109]. Other proposals include so-called accelerated weathering of limestone using CO_2-rich industrial flue-gas [116–119] (Box 8), and various electrochemical processes [109, 120–122] including a concept focused on Cl^- reduction via electrodialysis [123, 124].

Addition of alkalinity to the ocean helps to offset ocean acidification (the lowering of ocean pH due to anthropogenic CO_2 absorption) [106, 108], which is a major threat to marine ecosystems [106, 125, 126]. More relevant to this review, the increasing positive charge concentration due to OAE will force an increase in the negative charge concentration of the dominant anions [HCO_3^-] and [CO_3^{2-}], through a reduction in dissolved [CO_2]. Visualized in Fig. 2, the process drives a shift to the right along the X-axis, with increases in [HCO_3^-] and [CO_3^{2-}] along with a decrease in dissolved [CO_2]. The dissolved [CO_2] reduction implies a drop in pCO_2^w, and thus increases atmospheric CO_2 absorption. But the slowness of air-sea CO_2 equilibration then comes into play, which means that intensive OAE could cause severe temporary/regional CO_2 depletion, causing intense pCO_2^w gradients between well-mixed waters and the OAE source. In extreme cases, spots with CO_2 limitation of productivity might develop, when pCO_2^w locally falls below ~100 µatm, although mixing (and/or more diffuse addition) will alleviate that and overall productivity is thought to remain limited by nutrient and light availability [106, 127–131]. More significantly, OAE increases Ω, [HCO_3^-] and pH, and thus promotes calcification ($CaCO_3$ formation). Yet, calcification reduces alkalinity (Box 2 and Fig. 4), and thus offsets the desired effects of OAE. This, combined with further biogeochemical feedbacks—e.g. changes in the rain rate, including an enhanced carbonate pump as well as enhanced carbonate ballasting of POC—makes the net impacts of OAE difficult to quantify [106]. Much deeper understanding of this complex network of feedbacks is needed before such quantifications become feasible, and the expanded understanding needs to include also the impacts of addition of silica, Mg versus Ca, and trace elements through OAE [106]. Note also that OAE applied in an indiscriminate manner may trigger detrimental feedbacks that might offset (or worse) the CO_2 drawdown targeted with the OAE, which calls for careful monitoring of the seawater saturation state during the addition, so that the volume of alkalinity added can be adjusted accordingly [132].Renforth and Henderson [109] compared different ocean biogeochemical model experiments and found that, under certain hypothetical scenarios of pure alkalinity addition and ideal (immediate) dissolution of the added materials, ~166 GtC can be sequestered by 2100 [88], or that ~0.6 GtC can be sequestered each year for every Gt of olivine added to the surface ocean per year [110]. In the latter study, 57% of the sequestration arose from alkalinity increase, and 37% and 6% from the additions of iron and silicon derived from the olivine, respectively; but note that assuming ideal (immediate) dissolution is rather unrealistic in the case of olivine. A specific benefit of OAE is that it can (regionally at least) help keep the ocean at a higher carbonate (aragonite) saturation state, which will contribute to continued

Box 7. Silicate mineral weathering in essence follows reactions similar to that for olivine: $Mg_2SiO_4 + 4CO_2 + 4H_2O \rightarrow 2Mg^{2+} + 4HCO_3^- + H_4SiO_2$. Other silicate minerals have different cations instead of Mg (e.g. Ca) and thus produce different ions (e.g. Ca^{2+}), and/or clay minerals instead of dissolved silicic acid (H_4SiO_4). CO_2 sequestration using industrially produced lime uses the reverse calcination reaction $CaO + CO_2 \rightarrow CaCO_3$. The CaO would need to be industrially produced with CO_2 capture, to ensure a net CO_2 sequestration effect. In a natural state, throughout Earth history, CO_2 levels changed because of minor imbalances between removal of CO_2 by weathering and addition by volcanism, which over hundreds of thousands to millions of years changed the carbon inventory enough to influence climate (e.g. [30, 77, 109–113]). Reported natural global CO_2 consumption fluxes by chemical weathering of silicate rock range from 0.22 to 0.29 GtC y^{-1} [114, 115], so that an increase of the weathering rate by a factor of 100 would contribute significantly to anthropogenic carbon removal on timescales that are relevant to society. Therefore, the key challenge in artificial weathering methods for anthropogenic CO_2 sequestration, such as OAE, is to achieve acceleration of this process.

Box 8. The method of accelerated weathering of limestone using CO_2-rich industrial flue-gas [116–119] focuses on concentrated CO_2 that is captured at source from industrial emissions and is then fed through reactors with sea water and ground carbonate (e.g. industrial limestone or shell waste), to employ the $CaCO_3$ dissolution reaction $CaCO_3 + H_2O + CO_2 \rightarrow Ca^{2+} + 2HCO_3^-$. The water containing the reaction end products can then be distributed back into the ocean, where it helps restore seawater alkalinity and combat ocean acidification

coral reef health [109]. The survival of corals is under threat because we are getting uncomfortably close to their tolerances for thermal stress (+2°C) and carbonate-ion concentrations ($[CO_3^{2-}] = 200\,\mu mol\ kg^{-1}$, approximate aragonite saturation $\sim\Omega_{aragonite} = 3.3$; $[CO_2]^{atm} = 480$ ppm) [133].

Finally, Renforth and Henderson [109] discuss the longevity of C sequestration through OAE, and conclude that it might be of the order of hundreds to thousands of years. But—similar to Bach *et al.* [106]—they argue that too many uncertainties remain about potential feedback processes (including carbonate precipitation, which removes alkalinity), casting doubt on the robustness of this longevity range. This again emphasizes an urgent need for targeted research into the feedback processes, where the urgency arises from the fact that OAE seems to be a feasible, largely safe and potentially long-lasting method for CO_2 sequestration.

DEBUNKING FREQUENTLY ENCOUNTERED STATEMENTS/ARGUMENTS

Based on the reviewed material, we can now evaluate the statements or arguments that are frequently encountered in discussion groups, as listed in the introduction.

Statement 1: 'Oceanic CO_2 uptake with changing temperature may simply be calculated with physical solubility arguments'. This is incorrect. Such simple calculations may produce results that are off by as much as a factor 3–5. The complete suite of processes involved was found to be much more complicated, with major roles for (changes in) the temperature-sensitive Revelle factor (Box 1), the discrepancy between air–sea CO_2 equilibration timescales and circulation timescales (especially relevant if surface waters become involved in deep-water formation), and outgassing of biological pump-related CO_2 ($\Delta C_{gasx(bio)}$) from subsurface waters upon upwelling. Changing temperatures will therefore need to considered along with changing surface-water residence times and changing rates of deep-water formation, biological pump activity and upwelling (Box 3).

Statement 2: 'Carbonate formation should be promoted because it causes carbon drawdown'. This is incorrect. Carbonate precipitation causes a decrease in alkalinity and DIC, and an increase in pCO_2^w (Fig. 4), which is opposite to the expectation expressed in this statement. Organisms with carbonate hard body parts only cause net carbon drawdown because organic carbon is also formed and the soft tissue pump dominates following the 4:1 to 5:1 rain rate. Organisms with non-carbonate hard body parts (opal or organic compounds) are more effective at carbon drawdown. If, for some reason, approaches are desired that must only work with carbonate, then the focus for CO_2 removal must be on carbonate dissolution reactions (the exact opposite of the often proposed carbonate formation).

Statement 3: 'Ocean iron fertilization will draw down carbon and store it in increased fish populations (which are commercially interesting)'. This may be the case, but the impact on carbon drawdown is very limited. Expansion of fish stocks would be a one-time change only. Once the expansion has stabilized, a new steady state will exist where flux in equals flux out. Moreover, even under extreme assumptions of fish-stock expansion to 2 or 3 times the present-day global stock, such a one-time change would only represent a few percent of the oceanic C sequestration that is desired. The heavy lifting in productivity-based oceanic C sequestration must be done by continuous action of the soft tissue pump, driven by rapidly overturning single-celled plankton (Box 5).

Statement 4: 'Ocean iron fertilization has only positive (enriching) side-effects'. This is incorrect. Nutrients are used/depleted from surface waters and transported into deep water within organic matter sinking from successful iron fertilization regions. This causes surface waters downstream of these regions to become nutrient-depleted, with impacts on ecosystems that used to rely on the imported nutrients. Also, the nutrients in sinking organic matter will be released at depth through remineralization, and then remain absent from surface waters until upwelling circulation brings them back up (along with CO_2). Furthermore, oxygen is utilized during remineralization, and deep-water de-oxygenation underneath and downstream of iron fertilization regions poses a threat to communities that used to rely on the presence of sufficient oxygen. Finally, a host of insufficiently understood feedbacks can lead to production of other powerful greenhouse gases, as well as a rebound effect when iron fertilization is stopped, which would severely diminish the net benefits of the initial iron fertilization (Section 'Using the soft-tissue pump').

Statement 5: 'Enhanced primary production will be buried in sediments without major detrimental impacts'. This is a highly simplified view. First, only a fraction of productivity ever gets buried in the sediments, due to highly efficient remineralization in the water column, at the sea floor and within sediments. Second, organic carbon burial potential decreases greatly with increasing water depth, so that most of the burial occurs in shallow marine environments, and only a tiny fraction in the deep sea. Stimulating phytoplankton (or seaweed) growth therefore is only one critical part of the problem; the other critical part is how to ensure that this new production will actually reach the sea floor to stand a chance of being buried, rather than being remineralized within the water column. Third, the fraction of productivity lost to the sediments depends strongly on the type of ecosystem; some ecosystems (e.g. the Red Sea) have much lower proportions of carbon burial relative to new production than other ecosystems, so that not all regions are suitable for carbon removal through productivity enhancement. Moreover, in all cases, the increase in carbon burial that might be realized is only a small fraction of the additional productivity driven by fertilization, so that very large-scale fertilization is needed to trigger substantial increase in carbon burial fluxes. Optimization strategies may focus on: (i) fertilization in areas with anoxic waters/sediments because this promotes preservation of the organic flux to the sea floor and (ii) implementation in relatively shallow environments, given the great reduction in organic burial potential with increasing water depth. With respect to iron fertilization, this is problematic because hardly any sizeable HNLC regions overlie relatively shallow waters that are already anoxic or severely de-oxygenated because HNLC regions are by their very nature characterized by limited subsurface oxygen demand for remineralization, given their normally low organic matter flux. Creating anoxia in such regions poses a major threat to communities that used to rely on the presence of sufficient oxygen, and leads to feedbacks that can cause the release of other powerful greenhouse gases (Section 'Using the soft-tissue pump').

Statement 6: 'Impacts of regionally applied methods in the ocean can be confined to that region'. This is a complete misconception. The ocean is not a stationary body. It has both large-scale circulation that covers multi-centennial to millennial timescales, and medium to small-scale circulation (currents, eddies and turbulence) over all spatial scales and with typical timescales of seconds to centuries. All ocean properties get transported along in this dynamic environment. While being transported, both chemical and biological processes interact with many of

these properties (especially carbon, nutrients and oxygen). No regionally applied method can be contained to only regional impacts. This complex of lateral transport and mixing is also what makes it so difficult to verify the carbon drawdown efficiency of any method. Enrichment of one region may lead to ecosystem change (e.g. different communities/species), and there are potential downstream impacts in terms of environmental conditions (e.g. nutrient robbing, de-oxygenation and inorganic carbonate precipitation) and even foreign species invasion. The dynamic ocean environment also generates potential problems in CO_2-drawdown credit attribution (as well as further legal and societal implications), where one country's intervention (e.g. alkalinity enhancement) can lead to CO_2 drawdown in a downstream country's economic zone.

CONCLUSIONS

- The alkalinity of the ocean creates a massive increase in the ocean's capacity to store carbon, relative to a scenario without ocean alkalinity.
- Ocean warming causes decreases in both CO_2 solubility and the Revelle factor (B), which make the ocean less efficient at absorbing CO_2. Moreover, opposing influences of the two key air–sea gas exchange terms cause simple solubility-based arguments about carbon storage in the interior of the ocean to produce overestimates by a factor of 3–5.
- Surface-water production of $CaCO_3$ drives an increase rather than a decrease in surface-water pCO_2^w, but carbonate-bearing productivity remains of interest for carbon drawdown because the soft tissue pump component outperforms the carbonate pump component.
- Carbonate compensation (dissolution of sedimentary carbonate) is nature's ultimate mechanism for 'cleaning up' a major CO_2 perturbation, but it requires many tens of thousands of years and cannot conceivably be accelerated to timescales relevant to society. Hence, research concentrates on carbon storage (a) in the vast oceanic DIC reservoir with multi-centennial timescales and/or (b) through burial in sea-floor sediments with timescales up to millions of years. To achieve this, proposals focus on manipulation of either the soft tissue pump or ocean alkalinity.
- Many uncertainties remain with respect to soft tissue pump manipulation (notably, through ocean iron fertilization). These include: (i) feedbacks that partly or entirely offset the CO_2 sequestration gains, including production of N_2O or methane that would quickly erode the net greenhouse gas benefit (and cost efficiency) of iron fertilization; (ii) the likelihood of toxic algal bloom development; (iii) the potential for water-column de-oxygenation and (iv) side-effects to critical ecosystem services over a wider spatial domain due to, e.g., nutrient robbing.
- A key challenge in ocean alkalinity enhancement (OAE) is to develop the required mineral processing and distribution/dissolution mechanisms at volumes and timescales that are relevant to society. Estimates for the longevity (hundreds to thousands of years) and potential mass (tens to more than a hundred GtC by 2100) of C sequestration through OAE are highly relevant to the problem of anthropogenic CO_2 removal, but many uncertainties remain about feedback processes. There is specific urgency in accelerating research into these feedbacks for OAE because it seems to be a feasible, largely safe and potentially long-lasting method for CO_2 sequestration.
- As yet, the data and process understanding remain insufficient for predicting the plethora of underpinning processes, feedbacks and downstream impacts involved in oceanic methods for atmospheric carbon removal. Major international research investment is needed to address this gap in fundamental understanding, before well-intentioned, but potentially harmful, large-scale implementations are undertaken with insufficient scientific oversight.
- Finally, given the broad scope and potentially large spatial scales of feedbacks and impacts, it is imperative that large-scale oceanic methods for atmospheric carbon removal, once implemented, remain subject to ongoing and entirely independent, multi-national scientific monitoring, oversight and validation.

ACKNOWLEDGMENTS

I thank Lennart Bach, Jelle Bijma and Jack Middelburg for feedback on earlier drafts and formal review comments, and Lennart Bach, Jelle Bijma, Phil Boyd, Wally Broecker and Jimin Yu for stimulating carbon-cycle discussions over the years.

FUNDING

This study contributes to the Climate Recovery Institute, a broad collaboration on climate solutions (https://climaterecoveryinstitute.com.au).

CONFLICTS OF INTEREST STATEMENT

The author is an Editor of the journal and the article was therefore entirely handled and edited by another Associate Editor through peer review.

AUTHORS' CONTRIBUTIONS

Eelco Rohling (Conceptualization, Formal analysis, Funding acquisition, Investigation, Methodology, Project administration, Resources, Validation, Visualization, Writing—original draft and Writing—review & editing [equal]).

References

1. Meinshausen M, Lewis J, McGlade C *et al.* Realization of Paris Agreement pledges may limit warming just below 2°C. *Nature* 2022;**604**:304–9.
2. GESAMP. High level review of a wide range of proposed marine geoengineering techniques. *GESAMP Rep Stud* 2019;**98**:143.
3. National Academies of Sciences, Engineering, and Medicine. *Negative Emissions Technologies and Reliable Sequestration: A Research Agenda*. Washington, DC: The National Academies Press, 2019.
4. Rohling EJ. *Rebalancing Our Climate: The Future Starts Today*. New York, NY: Oxford University Press, 2021, 303.
5. Broecker WS, Peng TH. *Tracers in the Sea*. Palisades, NY: Lamont-Doherty Geological Observatory, Columbia University, 1982, 690.
6. Dickson AG. The carbon dioxide system in seawater: equilibrium chemistry and measurements. In: Riebesell U, Fabry VJ, Hansson L *et al.* (eds.), *Guide to Best Practices for Ocean*

Acidification Research and Data Reporting, Vol. **1.** Luxembourg: Publications Office of the European Union; 2010, 17–40.
7. Gieskes JM. The alkalinity-total carbon dioxide system in seawater. In: Goldberg ED (ed.), *The Sea*, Vol. **5**. New York, NY: Wiley, 1974, 123–51.
8. Gruber NI, Sarmiento JL. Large-scale biogeochemical–physical interactions in elemental cycles. *The Sea* 2002;**12**:337–99.
9. Middelburg JJ. *Marine Carbon Biogeochemistry. Springer Briefs in Earth System Sciences*. Cham, Switzerland: Springer, 2019, 57–75.
10. Middelburg JJ, Soetaert K, Hagens M. Ocean alkalinity, buffering and biogeochemical processes. *Rev Geophys* 2020;**58**: e2019RG000681.
11. Williams RG, Follows MJ. *Ocean Dynamics and the Carbon Cycle: Principles and Mechanisms*. Cambridge: Cambridge University Press, 2011, 404.
12. Zeebe RE, Wolf-Gladrow D. CO_2 in seawater: equilibrium, kinetics, isotopes. In: Halpern D (ed.), *Elsevier Oceanography Series*, Vol. **65**. Amsterdam, The Netherlands: Elsevier, 2001, 346.
13. Henry, W. Experiments on the quantity of gases absorbed by water, at different temperatures, and under different pressures. *Phil Trans Roy Soc Lond* 1803:**93**;29–43.
14. Bailey N, Papakyriakou TN, Bartels C *et al.* Henry's Law constant for CO_2 in aqueous sodium chloride solutions at 1 atm and sub-zero (Celsius) temperatures. *Mar Chem* 2018;**207**: 26–32.
15. Orr JC, Najjar RG, Aumont O, Bopp L, Bullister JL, Danabasoglu G, Doney SC, Dunne JP, Dutay JC, Graven H, Griffies SM. Biogeochemical protocols and diagnostics for the CMIP6 Ocean Model Intercomparison Project (OMIP). *Geoscientific Model Development* 2017 Jun 9;**10**(6):2169–99.
16. Weiss R. Carbon dioxide in water and seawater: the solubility of a non-ideal gas. *Mar Chem* 1974;**2**:203–15.
17. Jähne B, Haußecker H. Air–water gas exchange. *Ann Rev Fluid Mech* 1998;**30**:443–68.
18. Broecker WS, Peng TH. Gas exchange rates between air and sea. *Tellus* 1974;**26**:21–35.
19. Takahashi T, Feely RA, Weiss RF *et al.* Global air-sea flux of CO_2: an estimate based on measurements of sea–air pCO_2 difference. *Proc Nat Acad Sci* 1997;**94**:8292–9.
20. Takahashi T, Wanninkhof RH, Feely, RA *et al.* Net sea–air CO_2 flux over the global oceans: an improved estimate based on the sea–air pCO_2 difference. In: Nojiri Y (ed.), *Proceedings of the 2nd International Symposium on CO_2 in the Oceans*. Tsukuba, Japan: Center for Global Environmental Research, National Institute for Environmental Studies, Environmental Agency of Japan, 1999, 9–15.
21. Revelle R, Suess HE. Carbon dioxide exchange between atmosphere and ocean and the question of an increase of atmospheric CO_2 during the past decades. *Tellus* 1957:**9**;18–27.
22. Anderson LA. On the hydrogen and oxygen content of marine phytoplankton. *Deep-Sea Res I* 1995;**42**;1675–80.
23. Anderson LA, Sarmiento JL. Redfield ratios of remineralization determined by nutrient data analysis. *Glob Biogeochem Cycles* 1994;**8**;65–80.
24. Redfield AC, Ketchum BH, Richards FA. The influence of organisms on the composition of sea-water. In: Hill MN (ed.), *The Sea: Composition of Sea Water*, Vol. **2**. New York, NY: Wiley-Interscience, 1963, 26–77.
25. Takahashi T, Broecker WS, Langer S. Redfield ratio based on chemical data from isopycnal surfaces. *J Geophys Res Oceans* 1985;**90**:6907–24.
26. Bar-On YM, Phillips R, Milo R. The biomass distribution on Earth. *Proc Natl Acad Sci U S A* 2018;**115**:6506–11.
27. IPCC AR4. *Intergovernmental Panel on Climate Change. AR4 Climate Change 2007: The Physical Science Basis*. 2007. https://www.ipcc.ch/report/ar4/wg1/ (15 March 2023, last accessed).
28. Rohling EJ. *The Oceans: A Deep History*. Princeton, NJ: Princeton University Press, 2017, 272.
29. Sabine CL, Feely RA. The oceanic sink for carbon dioxide. In: Reay D, Hewitt N, Grace J *et al.* (eds). *Greenhouse Gas Sinks*, 2007, 31–49.
30. Rohling EJ. *The Climate Question: Natural Cycles, Human Impact, Future Outlook*. New York, NY: Oxford University Press, 2019, 162.
31. Hales B. Respiration, dissolution, and the lysocline. *Paleoceanography* 2003:**18**;1099.
32. Wagner S, Schubotz F, Kaiser K *et al.* Soothsaying DOM: a current perspective on the future of oceanic dissolved organic carbon. *Front Mar Sci* 2020;**7**:341.
33. Berner RA. Burial of organic carbon and pyrite sulfur in the modern ocean; its geochemical and environmental significance. *Am J Sci* 1982;**282**;451–73.
34. Archer DE. An atlas of the distribution of calcium carbonate in sediments of the deep sea. *Glob Biogeochem Cycles* 1996;**10**: 159–74.
35. Yu J, Anderson RF, Rohling EJ. Deep ocean carbonate chemistry and glacial–interglacial atmospheric CO_2 changes. *Oceanography* 2014;**27**:16–25.
36. Frankignoulle M, Canon C, Gattuso JP. Marine calcification as a source of carbon dioxide: positive feedback of increasing atmospheric CO_2. *Limnol Oceanogr* 1994;**39**:458–46.
37. Berger WH. Sedimentation of planktonic foraminifera. *Mar Geol* 1971;**11**:325–58.
38. Broecker WS, Takahashi T. Calcium carbonate precipitation on the Bahama Banks. *J Geophys Res* 1966;**71**:1575–602.
39. Cloud PE. Carbonate precipitation and dissolution in the marine environment. *Chem Oceanogr* 1965;**2**:127–58.
40. Müller G, Börker J, Sluijs A *et al.* Detrital carbonate minerals in Earth's element cycles. *Glob Biogeochem Cycles* 2022;**36**: e2021GB007231.
41. Berger WH. Biogenous deep-sea sediments: fractionation by deep-sea circulation. *Geol Soc Am Bull* 1970;**81**:1385–402.
42. Li YH, Takahashi T, Broecker WS. Degree of saturation of $CaCO_3$ in the oceans. *J Geophys Res* 1969;**74**:5507–25.
43. Milliman JD. Production and accumulation of calcium carbonate in the ocean: budget of a nonsteady state. *Glob Biogeochem Cycles* 1993;**7**:927–57.
44. Milliman JD, Droxler AW. Neritic and pelagic carbonate sedimentation in the marine environment: ignorance is not bliss. *Geol Rundsch* 1996;**85**:496–504.
45. Murnane RJ, Sarmiento JL, Le Quéré C. Spatial distribution of air-sea CO_2 fluxes and the interhemispheric transport of carbon by the oceans. *Glob Biogeochem Cycles* 1999;**13**:287–305.
46. Volk T, Hoffert MI. Ocean carbon pumps: analysis of relative strengths and efficiencies in ocean-driven atmospheric CO_2 changes. In: Sundquist ET, Broecker WS (eds.), *The Carbon Cycle and Atmospheric CO2: Natural Variations Archean to Present, Geophysical Monograph Series*, Vol. **32**. Hoboken, NJ: Wiley, 1985; 99–110.
47. Takahashi T, Olafsson J, Goddard JG *et al.* Seasonal variation of CO_2 and nutrients in the high-latitude surface oceans: a comparative study. *Glob Biogeochem Cycles* 1993;**7**:843–78.
48. Armstrong RA, Lee C, Hedges JI *et al.* A new, mechanistic model for organic carbon fluxes in the ocean based on the

quantitative association of POC with ballast minerals. *Deep Sea Res II: Top Stud Oceanogr* 2001;**49**:219–36.
49. Klaas C, Archer DE. Association of sinking organic matter with various types of mineral ballast in the deep sea: implications for the rain ratio. *Glob Biogeochem Cycles* 2002:**16**;1116.
50. Sabine CL, Tanhua T. Estimation of anthropogenic CO_2 inventories in the ocean. *Ann Rev Mar Sci* 2010;**2**:269–92.
51. Hauck J, Zeising M, Le Quéré C *et al.* Consistency and challenges in the ocean carbon sink estimate for the global carbon budget. *Front Mar Sci* 2020;**7**:571720.
52. Barker S, Ridgwell A. Ocean acidification. *Nat Educ Knowl* 2012; **3**:21.
53. Boudreau BP, Middelburg JJ, Meysman FJR. Carbonate compensation dynamics. *Geophys Res Lett* 2010;**37**:L03603.
54. He H, Li Y, Wang S, Ma Q *et al.* A high precision method for calcium determination in seawater using ion chromatography. *Front Mar Sci* 2020;**7**:231.
55. Zeebe RE, Westbroek PA. A simple model for the $CaCO_3$ saturation state of the ocean: the "Strangelove," the "Neritan," and the "Cretan" ocean. *Geochem Geophys Geosyst* 2003;**4**:1104.
56. Wolf-Gladrow DA, Zeebe RE, Klaas C *et al.* Total alkalinity: the explicit conservative expression and its application to biogeochemical processes. *Mar Chem* 2007;**106**:287–300.
57. Schink DR, Guinasso NL Jr. Modeling the influence of bioturbation and other processes on carbonate dissolution on the sea floor. In: Anderson NR, Malahoff A (eds.), *The Fate of Fossil Fuel CO2 in the Oceans*. New York, NY: Plenum, 1977, 375–99.
58. Takahashi T, Broecker WS. Mechanisms for calcite dissolution on the sea floor. In: Anderson NR, Malahoff A (eds.), *The Fate of Fossil Fuel CO2 in the Oceans*. New York, NY: Plenum, 1977, 455–77.
59. Tyrrell T. Calcium carbonate cycling in future oceans and its influence on future climates. *J Plankton Res* 2008;**30**:141–156.
60. Broecker WS. A need to improve reconstructions of the fluctuations in the calcite compensation depth over the course of the Cenozoic. *Paleoceanography* 2009;**23**:PA1204.
61. Kennett JP. *Marine Geology*. Englewood Cliffs, NJ: NJ Prentice Hall, 1982, 813.
62. Morse JM, Mackenzie FT. Geochemistry of sedimentary carbonates. *Developments in Sedimentology*, Vol. **48**. Amsterdam, The Netherlands: Elsevier, 1990, 707.
63. Goodwin P, Ridgwell A. Ocean-atmosphere partitioning of anthropogenic carbon dioxide on multimillennial timescales. *Glob Biogeochem Cycles* 2010;**24**:GB2014.
64. Lord NS, Ridgwell A, Thorne MC *et al.* An impulse response function for the "long tail" of excess atmospheric CO_2 in an Earth system model. *Glob Biogeochem Cycles* 2016;**30**:2–17.
65. Ridgwell A, Hargreaves JC. Regulation of atmospheric CO_2 by deep-sea sediments in an Earth system model. *Glob Biogeochem Cycles* 2007;**21**:GB2008.
66. Sulpis O, Boudreau BP, Mucci A *et al.* Current $CaCO_3$ dissolution at the seafloor caused by anthropogenic CO_2. *Proc Natl Acad Sci U S A* 2018;**115**:11700–5.
67. Ho TY, Quigg A, Finkel ZV *et al.* The elemental composition of some marine phytoplankton 1. *J Phycol* 2003:**39**;1145–59.
68. Horner TJ, Little SH, Conway TM *et al.* Bioactive trace metals and their isotopes as paleoproductivity proxies: an assessment using GEOTRACES-era data. *Glob Biogeochem Cycles* 2021;**35**: e2020GB006814.
69. Lauderdale JM, Braakman R, Forget G *et al.* Microbial feedbacks optimize ocean iron availability. *Proc Natl Acad Sci U S A* 2020; **117**:4842–9.
70. Martin JH. Glacial–interglacial CO_2 change: the iron hypothesis. *Paleoceanography* 1990;**5**:1–3.
71. Martin JH, Fitzwater SE. Iron deficiency limits phytoplankton growth in the north-east Pacific subarctic. *Nature* 1988;**331**:341–3.
72. Raven JA, Falkowski PG. Oceanic sinks for atmospheric CO_2. *Plant Cell Environ* 1999;**22**:741–55.
73. Wallace D, Law C, Boyd P *et al. Ocean Fertilization: A Scientific Summary for Policy Makers*. Paris: IOC/UNESCO (IOC/BRO/2010/ 2), 2010, 18.
74. Williamson P, Wallace DW, Law CS *et al.* Ocean fertilization for geoengineering: a review of effectiveness, environmental impacts and emerging governance. *Process Saf Environ Prot* 2012;**90**:475–88.
75. Yoon JE, Yoo KC, Macdonald AM *et al.* Reviews and syntheses: ocean iron fertilization experiments–past, present, and future looking to a future Korean Iron Fertilization Experiment in the Southern Ocean (KIFES) project. *Biogeosciences* 2018;**15**:5847–89.
76. Moore CM, Mills MM, Arrigo KR *et al.* Processes and patterns of oceanic nutrient limitation. *Nat Geosci* 2013;**6**:701–10.
77. Wallmann K, Aloisi G. The global carbon cycle: geological processes. In: Knoll AH, Canfield DE, Konhauser KO (eds.), *Fundamentals of Geobiology*, Hoboken, NJ: John Wiley & Sons, 2012, 20–35.
78. Hayes CT, Costa KM, Anderson RF *et al.* Global ocean sediment composition and burial flux in the deep sea. *Glob Biogeochem Cycles* 2021;**35**:e2020GB006769.
79. Boscolo-Galazzo F, Crichton KA, Barker S *et al.* Temperature dependency of metabolic rates in the upper ocean: a positive feedback to global climate change? *Glob Planet Change* 2018; **170**:201–12.
80. Ruvalcaba Baroni I, Palastanga V, Slomp CP. Enhanced organic carbon burial in sediments of oxygen minimum zones upon ocean deoxygenation. *Front Mar Sci* 2020;**6**:839.
81. Rogelj J, Den Elzen M, Höhne N *et al.* Paris agreement climate proposals need a boost to keep warming well below 2°C. *Nature* 2016;**534**:631–9.
82. Hansen J, Kharecha P, Sato M *et al.* Assessing "dangerous climate change": required reduction of carbon emissions to protect young people, future generations and nature. *PLoS ONE* 2013;**8**:e81648.
83. Hansen J, Sato M, Kharecha P *et al.* Young people's burden: requirement of negative CO_2 emissions. *Earth Syst Dyn* 2017;**8**: 577–616.
84. Buss W, Yeates K, Rohling EJ *et al.* Enhancing natural cycles in agro-ecosystems to boost plant carbon capture and soil storage. *Oxf Open Clim Change* 2021;**1**:kgab006.
85. Buss W, Wurzer C, Manning DA *et al.* Mineral-enriched biochar delivers enhanced nutrient recovery and carbon dioxide removal. *Commun Earth Environ* 2022;**3**:67.
86. Oschlies A, Koeve W, Rickels W *et al.* Side effects and accounting aspects of hypothetical large-scale Southern Ocean iron fertilization. *Biogeosciences* 2010;**7**:4017–35.
87. Fuhrman JA, Capone DG. Possible biogeochemical consequences of ocean fertilization. *Limnol Oceanogr* 1991;**36**:1951–9.
88. Keller DP, Feng EY, Oschlies A. Potential climate engineering effectiveness and side effects during a high carbon dioxide-emission scenario. *Nat Commun* 2014;**5**:3304.
89. Sarmiento JL, Orr JC. Three-dimensional simulations of the impact of Southern Ocean nutrient depletion on atmospheric CO_2 and ocean chemistry. *Limnol Oceanogr* 1991;**36**:1928–0.
90. Gnanadesikan A, Sarmiento JL, Slater RD. Effects of patchy ocean fertilization on atmospheric carbon dioxide and biological production. *Glob Biogeochem Cycles* 2003;**17**:1050.
91. Iversen MH, Ploug H. Ballast minerals and the sinking carbon flux in the ocean: carbon-specific respiration rates and sinking

velocity of marine snow aggregates. *Biogeosciences* 2010;**7**: 2613–24.
92. Ploug H, Iversen MH, Fischer G. Ballast, sinking velocity, and apparent diffusivity within marine snow and zooplankton fecal pellets: implications for substrate turnover by attached bacteria. *Limnol Oceanogr* 2008;**53**:1878–86.
93. Ploug H, Iversen MH, Koski M *et al.* Production, oxygen respiration rates, and sinking velocity of copepod fecal pellets: direct measurements of ballasting by opal and calcite. *Limnol Oceanogr* 2008;**53**:469–76.
94. van der Jagt H. The role of zooplankton and mineral ballasting in the biological carbon pump. Ph.D. Thesis, University of Bremen, 2019. doi:10.26092/elib/63 (15 March 2023, last accessed).
95. Sarmiento JL, Slater RD, Dunne J *et al.* Efficiency of small scale carbon mitigation by patch iron fertilization. *Biogeosciences* 2010;**7**:3593–624.
96. Xie Y, Tamsitt V, Bach LT. Localizing the southern ocean biogeochemical divide. *Geophys Res Lett* 2022;**49**:e2022GL098260.
97. Evans M. Climate fix? 'Fertilizing' oceans with iron unlikely to sequester more carbon. *Mongabay Series: Sea Change* 2020, **4** March. https://news.mongabay.com/2020/03/climate-fix-fertilizing-oceans-with-iron-unlikely-to-sequester-more-carbon/ (15 March 2023, last accessed)
98. Chalk TB, Hain MP, Foster GL *et al.* Causes of ice age intensification across the Mid-Pleistocene Transition. *Proc Nat Acad Sci* 2017;**114**:13114–9.
99. Yu J, Menviel L, Jin ZD *et al.* Sequestration of carbon in the deep Atlantic during the last glaciation. *Nat Geosci* 2016;**9**:319–24.
100. Dutkiewicz S, Follows MJ, Parekh P. Interactions of the iron and phosphorus cycles: a three-dimensional model study. *Glob Biogeochem Cycles* 2005;**19**:GB1021.
101. NIWA. 2010. Iron Fertilisation. https://niwa.co.nz/iron-fertilisation (15 March 2023, last accessed).
102. Royal Society. *Geoengineering the Climate: Science, Governance and Uncertainty*. London: The Royal Society, 2009, 84.
103. Jin X, Gruber N. Offsetting the radiative benefit of ocean iron fertilization by enhancing N_2O emissions. *Geophys Res Lett* 2003;**30**:2249.
104. Silver MW, Bargu S, Coale SL *et al.* Toxic diatoms and domoic acid in natural and iron enriched waters of the oceanic Pacific. *Proc Natl Acad Sci U S A* 2010;**107**:20762–7.
105. Trick CG, Bill BD, Cochlan WP *et al.* Iron enrichment stimulates toxic diatom production in high-nitrate, low-chlorophyll areas. *Proc Natl Acad Sci U S A* 2010;**107**:5887–92.
106. Bach LT, Gill SJ, Rickaby RE *et al.* CO_2 removal with enhanced weathering and ocean alkalinity enhancement: potential risks and co-benefits for marine pelagic ecosystems. *Front Clim* 2019;**1**:7.
107. Kheshgi HS. Sequestering atmospheric carbon dioxide by increasing ocean alkalinity. *Energy* 1995;**20**:915–22.
108. Köhler P, Hartmann J, Wolf-Gladrow DA. Geoengineering potential of artificially enhanced silicate weathering of olivine. *Proc Natl Acad Sci U S A* 2010;**107**:20228–33.
109. Renforth P, Henderson G. Assessing ocean alkalinity for carbon sequestration. *Rev Geophys* 2017;**55**:636–74.
110. Hauck J, Köhler P, Wolf-Gladrow D, Völker C. Iron fertilisation and century-scale effects of open ocean dissolution of olivine in a simulated CO2 removal experiment. Environmental Research Letters 2016;**11**(2):024007.
111. Berner RA, Lasaga AC, Garrels RM. Carbonate-silicate geochemical cycle and its effect on atmospheric carbon dioxide over the past 100 million years. *Am J Sci* 1983;**283**:641–83.
112. Garrels RM, Perry EA. Cycling of carbon, sulphur, and oxygen through geologic time. In: Goldberg ED (ed.), *The Sea*, Vol. **5**. New York, NY: Wiley, 1974, 303–36.
113. Gernon TM, Hincks TK, Merdith AS *et al.* Global chemical weathering dominated by continental arcs since the mid-Palaeozoic. *Nat Geosci* 2021;**14**:690–6.
114. Gaillardet J, Dupré B, Louvat P *et al.* Global silicate weathering and CO2 consumption rates deduced from the chemistry of large rivers. *Chem Geol* 1999; **159**: 3–30.
115. Hartmann J, Jansen N, Dürr HH *et al.* Global CO_2-consumption by chemical weathering: what is the contribution of highly active weathering regions? *Glob Planet Change* 2009;**69**:185–94.
116. Langer WH, Juan CA, Rau GH *et al.* Accelerated weathering of limestone for CO_2 mitigation opportunities for the stone and cement industries. In: *SME Annual Meeting and Exhibit and CMA's 111th National Western Mining Conference, Denver, CO*, Vol. **1**. United States Geological Survey Publications Warehouse. 2009, 310–5.
117. Rau GH. CO_2 mitigation via capture and chemical conversion in seawater. *Environ Sci Technol* 2011;**45**:1088–92.
118. Rau GH, Caldeira K. Enhanced carbonate dissolution: a means of sequestering waste CO_2 as ocean bicarbonate. *Energy Convers Manag* 1999;**40**:1803–13.
119. Rau GH, Knauss KG, Langer WH *et al.* Reducing energy-related CO_2 emissions using accelerated weathering of limestone. *Energy* 2007;**32**:1471–7.
120. House KZ, House CH, Schrag DP *et al.* Electrochemical acceleration of chemical weathering as an energetically feasible approach to mitigating anthropogenic climate change. *Environ Sci Technol* 2007;**41**:8464–70.
121. Rau GH. Electrochemical splitting of calcium carbonate to increase solution alkalinity: implications for mitigation of carbon dioxide and ocean acidity. *Environ Sci Technol* 2008;**42**: 8935–40.
122. Rau GH, Carroll SA, Bourcier WL *et al.* Direct electrolytic dissolution of silicate minerals for air CO_2 mitigation and carbon-negative H_2 production. *Proc Natl Acad Sci U S A* 2013;**110**:10095–100.
123. de Lannoy CF, Eisaman MD, Jose A *et al.* Indirect ocean capture of atmospheric CO_2: part I. prototype of a negative emissions technology. *Int J Greenh Gas Control* 2018;**70**:243–53.
124. Eisaman MD, Rivest JL, Karnitz SD *et al.* Indirect ocean capture of atmospheric CO_2: part II. Understanding the cost of negative emissions. *Int J Greenh Gas Control* 2018;**70**:254–61.
125. Doney SC, Fabry VJ, Feely RA *et al.* Ocean acidification: the other CO_2 problem. *Ann Rev Mar Sci* 2009;**1**;169–92.
126. Gattuso JP, Magnan A, Billé R *et al.* Contrasting futures for ocean and society from different anthropogenic CO_2 emissions scenarios. *Science* 2015;**349**:aac4722.
127. Bach LT, Riebesell U, Schulz KG. Distinguishing between the effects of ocean acidification and ocean carbonation in the coccolithophore *Emiliania huxleyi*. *Limnol Oceanogr* 2011;**56**: 2040–50.
128. Goldman JC. Inorganic carbon availability and the growth of large marine diatoms. *Mar Ecol Prog Ser* 1999;**180**:81–91.
129. Hansen PJ. Effect of high pH on the growth and survival of marine phytoplankton: implications for species succession. *Aqua Microb Ecol* 2002;**28**:279–88.
130. Riebesell U, Wolf-Gladrow DA, Smetacek V. Carbon dioxide limitation of marine phytoplankton growth rates. *Nature* 1993; **361**:249–51.

131. Sett S, Bach LT, Schulz KG *et al.* Temperature modulates coccolithophorid sensitivity of growth, photosynthesis and calcification to increasing seawater pCO_2. *PLoS ONE* 2014;**9**:e88308.
132. Moras CA, Bach LT, Cyronak T *et al.* Ocean alkalinity enhancement–avoiding runaway $CaCO_3$ precipitation during quick and hydrated lime dissolution. *Biogeosciences* 2022;**19**:3537–57.
133. Hoegh-Guldberg O, Poloczanska ES, Skirving W *et al.* Coral reef ecosystems under climate change and ocean acidification. *Front Mar Sci* 2017;**4**:158.
134. Iversen MH, Robert ML. Ballasting effects of smectite on aggregate formation and export from a natural plankton community. *Mar Chem* 2015;**175**:18–27.